Journal of Elasticity
https://doi.org/10.1007/s10659-024-10102-8

RESEARCH

Mechanics and Thermodynamics of Contractile Entropic Biopolymer Networks

Antoine Jallon[1] · **Pierre Recho**[1] · **Jocelyn Étienne**[1]

Received: 13 May 2024 / Accepted: 1 December 2024

Abstract
Contractile biopolymer networks, such as the actomyosin meshwork of animal cells, are ubiquitous in living organisms. The active gel theory, which provides a thermodynamic framework for these materials, has been mostly used in conjunction with the assumption that the microstructure of the biopolymer network is based on rigid rods. However, experimentally, crosslinked actin networks exhibit entropic elasticity. Here we combine an entropic elasticity kinetic theory, in the spirit of the Green and Tobolsky model of transiently crosslinked networks, with an active flux modelling biological activity. We determine this active flux by applying Onsager reciprocal relations to the corresponding microscopic dynamics. We derive the macroscopic active stress that arises from the resulting dynamics and obtain a closed-form model of the macroscopic mechanical behaviour. We show how this model can be rewritten using the framework of multiplicative deformation gradient decomposition, which is convenient for the resolution of such problems.

Keywords Actin · Myosin · Cytoskeleton · Active matter · Deformation gradient decomposition

Mathematics Subject Classification 92C10 · 74A60 · 76A10

1 Introduction

Active matter comprises a wide range of structures of mechanical relevance and features numerous means to perform mechanical work with and within them [1]. Among those, within the animal kingdom, biopolymer networks endowed with the ability to self-contract are arguably the most pervasive, both inside the cells and outside of them. Muscle contraction constitutes a classical example of this. It can be idealised as the relative sliding of parallelly-organised filaments of actin and myosin, actuated by the conformation change of the myosin, which itself is powered by the energy released by ATP hydrolysis [2, 3]. Actin and myosin are also essential players of the cytoskeleton. They are involved in an extensive range of active mechanical behaviours of cells [4–6], where they form a thin crosslinked network apposed to the plasma membrane [7], called the *actomyosin* cortex. The very rich repertoire of

✉ J. Étienne
jocelyn.etienne@univ-grenoble-alpes.fr

[1] Univ. Grenoble Alpes–CNRS, LIPHY, Grenoble, France

contractile networks has also been explored in vitro using purified gels of biological proteins [8–10]. While in vitro gels have properties that are distinct from those of cytoskeletal actomyosin, the geometry of the microstructure and the origins of active stress bear interesting similarities.

Continuum modelling approaches have been able to reproduce a number of the behaviours of the actomyosin cytoskeleton by the introduction of an active stress as a driving force within a liquid-like material modelling the network [11]. This active stress can be interpreted as a dynamic prestress [12], allowing to draw analogies with the residual stress which is observed in solid-like tissue [13, 14]. The theory of active gels [15, 16], drawing from the hydrodynamics of suspensions of orientable objects endowed with active stresses [17], has provided a sound thermodynamic framework for the generation of this active stress by molecular motors. A link has been done with materials whose microstructure relies on rigid filaments [18–20]. Actin filaments are semiflexible, however, to the difference of lamellipodium-like networks [21], the elasticity of crosslinked networks has been shown to be of entropic nature [22]. It is thus interesting to consider in what measure the entropic elasticity of the microstructure modifies the constitutive relations of active biopolymer networks.

Here, we consider a microstructure of freely-jointed chains, exhibiting entropic elasticity, which form a percolating network through high-affinity but reversible binding. In addition to affine deformations, we allow for motion due to the action of active crosslinks, which model molecular motors. The thermodynamics of this system is then written within the constraints of this particular microstructure, which allows us to propose microscopic interpretations of the Onsager relations.

Section 2 presents the kinetic model, its thermodynamics and is concluded with a closed mechanical model. Section 3 introduces a multiplicative decomposition that allows to recover this model and is convenient for its resolution and for numerical approaches. Section 4 concludes the paper with two simple examples demonstrating the method.

2 A Kinetic Theory of Contractile Biopolymer Networks

2.1 Kinetics of Active Temporary Networks

In this section, we follow the approach of transiently crosslinked networks [23, 24] and combine it explicitly with an elastic dumbbell model [25–27] to describe the dynamics of unbound chains. This will make possible the interpretation of the dissipation in the next section. The other novelty here is the presence of an additional flux, which represents the active dynamics of the network. It is not specified in this section how this flux depends on other fields, this will be done in view of the thermodynamics of the system in Sect. 2.3, allowing us to reconcile phenomenological kinetic approaches [28] with generic thermodynamic considerations [15].

We consider the biopolymer network as an assembly of polymer molecules of idealised elastic freely-jointed chains in a viscous liquid (e.g. the cytosol). Each chains can be represented by an elastic dumbbell [27], that is, a spring joining two beads which can bind to beads of neighbouring molecules. For each chain, the end-to-end vector $\underset{\sim}{\boldsymbol{R}}(t) \in \mathbb{R}^3$, called *strand*, connects each of the dumbbell beads, see Fig. 1.

We assume a high affinity between the chains and that consequently, a large connected component of chains forms a macroscopic network. Within this percolated component, each "bound" strand $\underset{\sim}{\boldsymbol{R}}_{\mathrm{b}}$ is assumed to deform affinely with the network. Thus, if the macroscopic

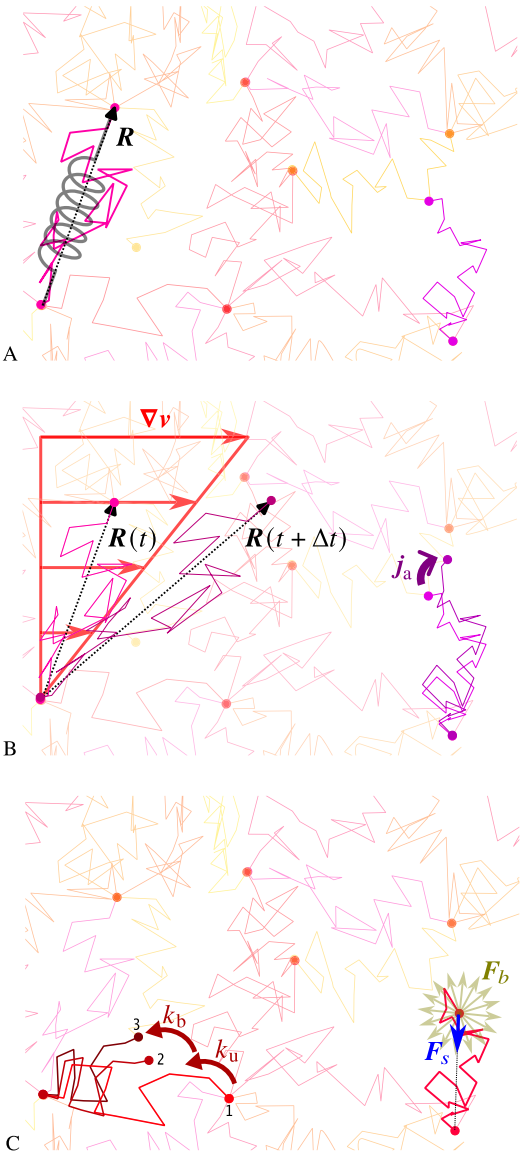

Fig. 1 Network model. **A**, Chains made of a finite number of freely-jointed segments. Each is described by an end-to-end vector $\underset{\sim}{\boldsymbol{R}}$ and can be modelled as a spring. They can connect to other chains at their ends. **B**, If a global deformation $\underset{\sim}{\nabla}\underset{\sim}{\boldsymbol{v}}$ exists, bound chains are affinely deformed, Eq. (1). The additional active flux $\underset{\sim}{\boldsymbol{j}}_{\mathrm{a}}$ is described in Sect. 2.3. **C**, Unbound end of a chain is submitted to spring force $\underset{\sim}{\boldsymbol{F}}_s$ and to a Brownian force $\underset{\sim}{\boldsymbol{F}}_b$. Unbound chains relax extremely fast to a configuration where those forces balance. Bound ends (configuration 1) unbind at rate k_{u} and the chain thus relaxes (configuration 2). They will then quickly rebind at rate k_{b} (configuration 3) but do so in their relaxed state

velocity gradient $\underset{\approx}{\boldsymbol{\ell}}^{\mathsf{T}}$ varies over distances much greater than the typical length of $\underset{\sim}{\boldsymbol{R}}_{\mathrm{b}}$, the dynamic of $\underset{\sim}{\boldsymbol{R}}_{\mathrm{b}}$ is given by:

$$\dot{\underset{\sim}{\boldsymbol{R}}}_{\mathrm{b}} = \underset{\approx}{\boldsymbol{\ell}} \cdot \underset{\sim}{\boldsymbol{R}}_{\mathrm{b}} + \underset{\sim}{\boldsymbol{j}}_{\mathrm{a}}. \tag{1}$$

Here $\underset{\sim}{\boldsymbol{j}}_{\mathrm{a}}$ represents some active process that remodels the network, yet unspecified, the case of passive transiently crosslinked networks being $\underset{\sim}{\boldsymbol{j}}_{\mathrm{a}} = \underset{\sim}{\boldsymbol{0}}$.

However, transiently, one of the beads in a dumbbell can disconnect from this network, undergo different dynamics, and then reconnect to it. The rate constants governing connection and disconnection will be set such that these transients are of short duration, one conse-

quence being that we do not need to consider the quadratically rare cases where both beads disconnect. When one of the beads is disconnected, it is subjected to the internal spring force $\underset{\sim}{\boldsymbol{F}}_s$ exerted by the chain, which remains bound to the network by the other bead, and to the Brownian force $\underset{\sim}{\boldsymbol{F}}_b$ due to the thermal fluctuations in the liquid. This can be expressed in a stochastic differential equation, called a Langevin equation, which governs the dynamics of the "unbound" strand $\underset{\sim}{\boldsymbol{R}}_{\mathrm{u}}$:

$$\zeta(\dot{\underset{\sim}{\boldsymbol{R}}}_{\mathrm{u}} - \underset{\approx}{\boldsymbol{\ell}} \cdot \underset{\sim}{\boldsymbol{R}}_{\mathrm{u}}) = \underset{\sim}{\boldsymbol{F}}_s + \underset{\sim}{\boldsymbol{F}}_b, \tag{2}$$

where ζ is the drag coefficient of the bead in the fluid. The liquid is considered to have the same velocity locally as the network, thus the viscous drag force on the free end of the chain is proportional to its velocity relative to $\underset{\approx}{\boldsymbol{\ell}} \cdot \underset{\sim}{\boldsymbol{R}}_{\mathrm{u}}$, where we have again considered that the variations of $\underset{\approx}{\boldsymbol{\ell}}$ are on a larger spatial scale than the typical $|\underset{\sim}{\boldsymbol{R}}_{\mathrm{u}}|$.

Up to a factor two on the drag coefficient ζ (due to the bound state of one of the beads), this is the same Langevin equation as the one used to derive dumbbell models [25–27], and the expressions of the forces are the same:

$$\underset{\sim}{\boldsymbol{F}}_b = \sqrt{2\zeta k_B T}\,\underset{\sim}{\boldsymbol{\eta}}(t), \tag{3}$$

$$\underset{\sim}{\boldsymbol{F}}_s = -\kappa \underset{\sim}{\boldsymbol{R}}_u. \tag{4}$$

The form of $\underset{\sim}{\boldsymbol{F}}_b$, with k_B the Boltzmann constant, T the temperature and $\underset{\sim}{\boldsymbol{\eta}}$ an isotropic white noise is chosen to guarantee the equipartition of energy in the permanent regime [26] for the (passive) unbound phase. The strand stiffness $\kappa = 2k_B T\beta^2$ is normalized with the thermal energy where β^{-1} is a length proportional to the square root of the number of segments in the chain.

We now introduce the probability densities for a strand to be bound (resp. unbound) and of a certain length $\psi_{\mathrm{b,u}}(\boldsymbol{r}, t)\mathrm{d}\boldsymbol{r} = \mathrm{Prob}\{\mathrm{b,u}\} \cdot \mathrm{Prob}(r_i < \underset{\sim}{\boldsymbol{R}}(t) \cdot \underset{\sim}{\boldsymbol{e}}_i < r_i + \mathrm{d}r_i)$. The Fokker-Planck dynamics associated to the Langevin process (1)-(2) are described by a conservation equation for each of these probability densities, taking into account the 'probability current' defined by the Langevin process and the exchanges between the two states, bound and unbound. They take the form:

$$\frac{\partial \psi_{\mathrm{b}}}{\partial t} + \underset{\sim}{\nabla}_{\boldsymbol{r}} \cdot \left(\psi_{\mathrm{b}}(\underset{\approx}{\boldsymbol{\ell}} \cdot \underset{\sim}{\boldsymbol{r}} + \underset{\sim}{\boldsymbol{j}}_{\mathrm{a}})\right) = -k_{\mathrm{u}}\mathcal{K}_u(\psi_{\mathrm{u}}, \psi_{\mathrm{b}}), \tag{5a}$$

$$\frac{\partial \psi_{\mathrm{u}}}{\partial t} + \underset{\sim}{\nabla}_{\boldsymbol{r}} \cdot \left(\psi_{\mathrm{u}}\big(\underset{\approx}{\boldsymbol{\ell}} \cdot \underset{\sim}{\boldsymbol{r}} - (\kappa/\zeta)\underset{\sim}{\boldsymbol{r}}\big) - (k_B T/\zeta)\underset{\sim}{\nabla}_{\boldsymbol{r}}\psi_{\mathrm{u}}\right) = \quad k_{\mathrm{u}}\mathcal{K}_u(\psi_{\mathrm{u}}, \psi_{\mathrm{b}}), \tag{5b}$$

where the left hand sides are obtained in the absence of exchange terms between the bound and unbound states [29] and a reaction term $k_{\mathrm{u}}\mathcal{K}_u$ appears on the right hand side in order to model binding and unbinding. The characteristic time for this process is the unbinding rate k_{u}. In the sequel we will take the simplest possible reaction term, $\mathcal{K}_u = \psi_{\mathrm{b}} - (k_{\mathrm{b}}/k_{\mathrm{u}})\psi_{\mathrm{u}}$, with k_{b} a constant binding rate. Note that the total probability distribution of the two populations, $\psi = \psi_{\mathrm{u}} + \psi_{\mathrm{b}}$, is such that $\int_{\mathbb{R}^3} \psi \, \mathrm{d}\boldsymbol{r} = 1$.

We now consider the limit of low drag resistance to the motion of unbound chains: this corresponds to a fast relaxation to equilibrium, happening before a chain rebinds to the network, and thus $\zeta k_{\mathrm{b}}/\kappa \ll 1$. As already stated, the unbinding process is assumed to be slower than the binding one, $k_{\mathrm{u}} \lesssim k_{\mathrm{b}}$, which is necessary to obtain a large connected component forming the network. We additionally restrict ourselves to rates of flow which cannot exceed the binding rate, $|\underset{\approx}{\boldsymbol{\ell}}| \lesssim k_b$, to prevent mechanical rupture. Under these conditions, we

can then expand ψ_u as $\psi_\mathrm{u} = a_\mathrm{u}\psi_0 + O(\zeta k_\mathrm{b}/\kappa)$ where $\psi_0(\underset{\sim}{\boldsymbol{r}})$ is time-independent and solves Eq. (5b) to the first order, see Appendix A. The fraction of bound chains a_u is found to tend to a permanent regime value characterised by $\int_{\mathbb{R}^3} \mathcal{K}_u(\psi_\mathrm{u}, \psi_\mathrm{b})\,\mathrm{d}\boldsymbol{r} = 0$. For our choice of $\mathcal{K}_u$, this results in $a_\mathrm{u} = k_\mathrm{u}/(k_\mathrm{b} + k_\mathrm{u})$. We will often consider the case $k_\mathrm{u} \ll k_\mathrm{b}$, since this simplifies some of the expressions.

The time dependent part of ψ is thus reduced to ψ_b, and from Eq. (5a) we have:

$$\frac{\partial \psi_\mathrm{b}}{\partial t} + \underset{\sim}{\nabla}_{\boldsymbol{r}} \cdot \left(\psi_\mathrm{b}(\underset{\approx}{\boldsymbol{\ell}} \cdot \underset{\sim}{\boldsymbol{r}} + \underset{\sim}{\boldsymbol{j}}_\mathrm{a})\right) = -k_\mathrm{u}\mathcal{K}_0(\psi_\mathrm{b}) + O\left(\frac{\zeta k_\mathrm{b} k_\mathrm{u}}{\kappa}\right). \tag{6}$$

For $\underset{\sim}{\boldsymbol{j}}_\mathrm{a} = \underset{\sim}{\boldsymbol{0}}$ and since the first order approximation is $k_\mathrm{u}\mathcal{K}_0(\psi_\mathrm{b}) = k_\mathrm{u}\psi_\mathrm{b} - k_\mathrm{b}a_\mathrm{u}\psi_0$, Eq. (6) is the same Smoluchowski equation as found by [24] for ψ_b, this is known to lead to the upper-convected Maxwell constitutive equation for stress–strain relation [26, p. 168], with a relaxation time equal to k_u^{-1}. Note that the upper-convected Maxwell stress–strain relation, with relaxation time equal to ζ/κ, is also the result for unbound chains only, i.e. Eqs. (5b), with $\mathcal{K}_u = 0$ but finite ζ.

2.2 The Stress Tensor

Elastic forces in stretched polymer chains result in a stress in the network, which can be described using the distribution ψ and the spring force $\underset{\sim}{\boldsymbol{F}}_s$. The classical derivation of the stress tensor uses the procedure of integrating the forces exerted by this distribution of springs on an elementary volume, but the same result can be obtained using the virtual work principle [26, p. 33]. As will be seen below, this is useful in the context of active systems.

For our isothermal system, the total dissipation can be written as:

$$\mathcal{D} = \frac{\delta W}{\delta t} - \frac{\mathrm{d}\mathcal{F}}{\mathrm{d}t} \geq 0$$

where the terms are respectively the rate of work and the Gibbs free energy variations. The system is actually open, since an energy input from the outside maintains out of equilibrium a chemical reaction feeding the power strokes of molecular motors [30], which are modelled with the term $\underset{\sim}{\boldsymbol{j}}_\mathrm{a}$. When this reaction is maintained at a fixed distance from equilibrium, we include the energy exchange term with the environment in $\mathcal{F}$, as classically done in the active gel theory [15]. This will be specified in Sect. 2.3.

We now proceed to determine the rate of work. Let $\Omega(t)$ be the domain occupied by the material at time t. The trajectory of material points of the network is denoted $\underset{\sim}{\boldsymbol{x}} = \underset{\sim}{\boldsymbol{\chi}}(\underset{\sim}{\boldsymbol{X}}, t) \in \Omega(t)$ where $\underset{\sim}{\boldsymbol{X}} \in \Omega(0)$ is the initial position at time $t = 0$. We define the deformation gradient as $\underset{\approx}{\mathbf{F}}(\underset{\sim}{\boldsymbol{X}}, t) = \underset{\sim}{\nabla}_{\boldsymbol{X}}\underset{\sim}{\boldsymbol{\chi}}(\underset{\sim}{\boldsymbol{X}}, t)^\mathsf{T}$, with the convention $\underset{\sim}{\nabla}_{\boldsymbol{X}}\underset{\sim}{\boldsymbol{U}} = \sum_{i,j} \partial U_j/\partial X_i \underset{\sim}{\boldsymbol{e}}_i\underset{\sim}{\boldsymbol{e}}_j$. We follow the conventions of [27] among others, notably the outer (dyadic) product is implied between vectors, $\underset{\sim}{\boldsymbol{U}}\,\underset{\sim}{\boldsymbol{V}} = \sum_{i,j} U_i V_j \underset{\sim}{\boldsymbol{e}}_i\underset{\sim}{\boldsymbol{e}}_j$ while $\cdot$ denotes the scalar product of vectors, the tensor–vector product and the contracted product of second order tensors $\underset{\approx}{\mathbf{T}} \cdot \underset{\approx}{\mathbf{S}} = \sum_{i,j,k} T_{i,k}S_{k,j}\underset{\sim}{\boldsymbol{e}}_i\underset{\sim}{\boldsymbol{e}}_j$. Finally, : is the doubly contracted product, $\underset{\approx}{\mathbf{T}} : \underset{\approx}{\mathbf{S}} = \sum_{i,j} T_{i,j}S_{j,i}$.

The velocity is

$$\underset{\sim}{\boldsymbol{v}} = \frac{\partial \underset{\sim}{\boldsymbol{\chi}}}{\partial t}(\underset{\sim}{\boldsymbol{\chi}}^{-1}(\underset{\sim}{\boldsymbol{x}}, t), t),$$

and we identify $\underset{\approx}{\boldsymbol{\ell}} = \underset{\sim}{\nabla}_{\boldsymbol{x}}\underset{\sim}{\boldsymbol{v}}^\mathsf{T}$. To remain in the conditions above, it is assumed that $\underset{\approx}{\mathbf{F}}(\underset{\sim}{\boldsymbol{X}}, t)$ varies in space over distances much longer than the typical length of a strand $\underset{\sim}{\boldsymbol{R}}$. We assume that inertia and body forces acting on the system are negligible, leading to the momentum

balance equations:

$$\underset{\sim}{\nabla}_{\boldsymbol{x}} \cdot \underset{\approx}{\boldsymbol{\tau}} = \underset{\sim}{\mathbf{0}} \qquad \text{in } \Omega(t) \tag{7a}$$

$$\underset{\approx}{\boldsymbol{\tau}} \cdot \underset{\sim}{\boldsymbol{n}} = \underset{\sim}{\boldsymbol{f}}_{\text{ext}} \qquad \text{on } \partial\Omega(t) \tag{7b}$$

where $\underset{\sim}{\boldsymbol{f}}_{\text{ext}}$ are the external forces applied on the system's boundaries and $\underset{\approx}{\boldsymbol{\tau}}$ the Cauchy stress tensor.

Let us denote $\nu(\underset{\sim}{\boldsymbol{x}})$ the number of chains per unit volume within $\Omega(t)$. Mass conservation gives

$$\frac{\partial \nu}{\partial t} + \underset{\sim}{\nabla}_{\boldsymbol{x}} \cdot (\nu \underset{\sim}{\boldsymbol{v}}) = 0 \qquad \text{in } \Omega(t) \tag{8a}$$

$$\nu(\underset{\sim}{\boldsymbol{v}} - \underset{\sim}{\boldsymbol{v}}_b) \cdot \underset{\sim}{\boldsymbol{n}} = 0 \qquad \text{on } \partial\Omega(t) \tag{8b}$$

$$\nu(t=0) = \nu_0 \qquad \text{in } \Omega_0 = \Omega(0) \tag{8c}$$

where $\underset{\sim}{\boldsymbol{v}}_b(t)$ is the velocity of $\partial\Omega(t)$, which from the above has its normal component equal to $\underset{\sim}{\boldsymbol{v}}$.

The rate of work is equal to the work performed on the system's boundary, and from Eqs. (7a) and (7b) and using the symmetry of $\underset{\approx}{\boldsymbol{\tau}}$,

$$\frac{\delta W}{\delta t} = \int_{\partial\Omega(t)} \underset{\sim}{\boldsymbol{f}}_{\text{ext}} \cdot \underset{\sim}{\boldsymbol{v}}_b \, \mathrm{d}\boldsymbol{s} = \int_{\Omega(t)} \underset{\approx}{\boldsymbol{\tau}} : \underset{\approx}{\boldsymbol{d}} \, \mathrm{d}\boldsymbol{x} \tag{9}$$

with $\underset{\approx}{\boldsymbol{d}} = \frac{1}{2}(\underset{\approx}{\boldsymbol{\ell}} + \underset{\approx}{\boldsymbol{\ell}}^{\mathsf{T}})$.

We now write the Gibbs free energy of the whole system:

$$\mathcal{F} = \int_{\Omega(t)} \nu\varphi \, \mathrm{d}\boldsymbol{x}.$$

The specific free energy density φ can be decomposed as $\varphi = \varphi_{\mathrm{e}} + \varphi_{\mathrm{a}}$, where φ_{a} represents anelastic contributions, which we will relate to active processes in Sect. 2.3, and φ_{e} is the specific elastic free energy density. Following [26, p. 33], it is:

$$\nu\varphi_{\mathrm{e}} := \frac{1}{2}\nu\kappa \int_{\mathbb{R}^3} \psi(\underset{\sim}{\boldsymbol{r}}) \boldsymbol{r}^2 \, \mathrm{d}\boldsymbol{r},$$

where $\boldsymbol{r}^2 = \underset{\sim}{\boldsymbol{r}} \cdot \underset{\sim}{\boldsymbol{r}}$.

The free energy variations are:

$$\frac{\mathrm{d}\mathcal{F}}{\mathrm{d}t} = \int_{\Omega(t)} \left(\frac{\partial \nu}{\partial t}\varphi + \nu \frac{\partial \varphi}{\partial t} \right) \mathrm{d}\boldsymbol{x} = \int_{\Omega(t)} \nu \frac{\mathrm{d}\varphi}{\mathrm{d}t} \, \mathrm{d}\boldsymbol{x} \tag{10}$$

where we have used Eq. (8a) and one integration by parts.

Since in the limit $\zeta k_{\mathrm{b}}/\kappa \to 0$, ψ_{u} is time-independent, the elastic contributions to free energy density variations can be deduced from the Smoluchowski Eq. (6):

$$\begin{aligned}
\nu \frac{\mathrm{d}\varphi_{\mathrm{e}}}{\mathrm{d}t} &= \frac{1}{2}\nu\kappa \int_{\mathbb{R}^3} \frac{\partial \psi_{\mathrm{b}}}{\partial t} \boldsymbol{r}^2 \, \mathrm{d}\boldsymbol{r} \\
&\overset{\text{IbP}}{=} \frac{1}{2}\nu\kappa \int_{\mathbb{R}^3} \psi_{\mathrm{b}} (\underset{\sim}{\boldsymbol{r}} \cdot \underset{\sim}{\nabla}_{\boldsymbol{x}} \underset{\sim}{\boldsymbol{v}} + \underset{\sim}{\boldsymbol{j}}_{\mathrm{a}}) \cdot \underset{\sim}{\nabla}_{\boldsymbol{r}} \boldsymbol{r}^2 \, \mathrm{d}\boldsymbol{r} - \frac{1}{2}\nu\kappa k_{\mathrm{u}} \int_{\mathbb{R}^3} \mathcal{K}_0(\psi_{\mathrm{b}}) \boldsymbol{r}^2 \, \mathrm{d}\boldsymbol{r} \\
&= \nu\kappa \left(\langle \underset{\sim}{\boldsymbol{r}} \underset{\sim}{\boldsymbol{r}} \rangle_{\mathrm{b}} : \underset{\approx}{\boldsymbol{d}} + \langle \underset{\sim}{\boldsymbol{j}}_{\mathrm{a}} \cdot \underset{\sim}{\boldsymbol{r}} \rangle_{\mathrm{b}} - \frac{1}{2} k_{\mathrm{u}} \int_{\mathbb{R}^3} \mathcal{K}_0(\psi_{\mathrm{b}}) \boldsymbol{r}^2 \, \mathrm{d}\boldsymbol{r} \right)
\end{aligned}$$

where $\langle\cdot\rangle_\mathrm{b} = \int_{\mathbb{R}^3} \psi_\mathrm{b} \cdot \mathrm{d}\boldsymbol{r}$. It is thus the second moment of the distribution of bound strands, $\underset{\approx}{\mathbf{A}} = \langle \underset{\sim}{\boldsymbol{r}}\underset{\sim}{\boldsymbol{r}}\rangle_\mathrm{b}$, which is conjugated with the rate of strain $\underset{\approx}{\boldsymbol{d}}$. This tensor $\underset{\approx}{\mathbf{A}}$ is called the *microstructure (or texture) tensor* [31] of the network.

We are now in a position to identify the different terms in the dissipation,

$$\mathcal{D} = \mathcal{D}_\mathrm{w} + \mathcal{D}_\mathrm{r} + \mathcal{D}_\mathrm{a},$$

where the first term is a dissipation induced by the deformation rate:

$$\mathcal{D}_\mathrm{w} = \int_{\Omega(t)} \left(\underset{\approx}{\boldsymbol{\tau}} - \nu\kappa\underset{\approx}{\mathbf{A}}\right) : \underset{\approx}{\boldsymbol{d}}\, \mathrm{d}\boldsymbol{x},$$

the second term is a dissipation associated with the relaxation of chains via the unbinding–rebinding dynamics:

$$\mathcal{D}_\mathrm{r} = \frac{1}{2}\int_{\Omega(t)} \nu\kappa k_\mathrm{u} \int_{\mathbb{R}^3} \mathcal{K}_0(\psi_\mathrm{b})\boldsymbol{r}^2\, \mathrm{d}\boldsymbol{r}\, \mathrm{d}\boldsymbol{x}$$

and the third is the power balance of active processes:

$$\mathcal{D}_\mathrm{a} = -\int_{\Omega(t)} \nu\left(\frac{\mathrm{d}\varphi_\mathrm{a}}{\mathrm{d}t} + \kappa\langle \underset{\sim}{\boldsymbol{j}}_\mathrm{a}\cdot\underset{\sim}{\boldsymbol{r}}\rangle_\mathrm{b}\right)\mathrm{d}\boldsymbol{x}.$$

One can further decompose the stress term into deviatoric and isotropic components,

$$\mathcal{D}_\mathrm{w} = \int_{\Omega(t)} \left(\mathbf{dev}(\underset{\approx}{\boldsymbol{\tau}} - \nu\kappa\underset{\approx}{\mathbf{A}}) : \underset{\approx}{\boldsymbol{d}} + \frac{1}{3}\mathrm{tr}(\underset{\approx}{\boldsymbol{\tau}} - \nu\kappa\underset{\approx}{\mathbf{A}})\underset{\approx}{\mathbf{I}} : \underset{\approx}{\boldsymbol{d}}\right)\mathrm{d}\boldsymbol{x}.$$

In what follows we choose to treat the case of an incompressible material only, which yields $\underset{\approx}{\mathbf{I}} : \underset{\approx}{\boldsymbol{d}} = \underset{\sim}{\boldsymbol{\nabla}}\cdot\underset{\sim}{\boldsymbol{v}} = 0$ and cancels the second term of the integrand. This is enforced by a pressure p as a Lagrange multiplier. Following e.g. [27], we decompose the stress $\underset{\approx}{\boldsymbol{\tau}} = -p\underset{\approx}{\mathbf{I}} + \underset{\approx}{\boldsymbol{\sigma}}$ where $\underset{\approx}{\boldsymbol{\sigma}}$ is the so-called *extra stress tensor*. In order to guarantee $\mathcal{D}_\mathrm{w} \geq 0$, the extra stress tensor can then be chosen as $\underset{\approx}{\boldsymbol{\sigma}} = \nu\kappa(\underset{\approx}{\mathbf{A}} - \underset{\approx}{\mathbf{A}}_0) + 2\mu\underset{\approx}{\boldsymbol{d}}$, where μ introduces an additional dissipation not related with the microstructure, typically ascribed to a shear viscosity of the liquid bath. Incompressibility implies that isotropic terms in the stress are not contributing to the dissipation. We have thus introduced an arbitrary isotropic tensor $\underset{\approx}{\mathbf{A}}_0 = a_0\beta^{-2}\underset{\approx}{\mathbf{I}}$, and we will see in the next section that the relaxed state of the chains prescribes a nonzero a_0. We obtain

$$\mathcal{D}_\mathrm{w} = \int_{\Omega(t)} 2\mu\underset{\approx}{\boldsymbol{d}} : \underset{\approx}{\boldsymbol{d}}\, \mathrm{d}\boldsymbol{x} \geq 0,$$

thus only the liquid bath may contribute to a dissipation induced by the rate of deformation.

2.3 Active Terms: Molecular Motors as Crosslinks

We now turn to the modelling of the molecular motors. We have assumed that their effect was felt through a flux $\underset{\sim}{\boldsymbol{j}}_\mathrm{a}$ in the dynamics of bound chains, Eq. (1), since indeed myosin minifilaments are a crosslinking type of molecular motors which can actively displace their binding position along either of the actin filaments they are bound to during events called power-strokes [32]. We now investigate what form of $\underset{\sim}{\boldsymbol{j}}_\mathrm{a}$ is admissible from a close-to-equilibrium thermodynamics point of view.

The power-stroke process is driven by a chemical reaction in which ATP hydrolysis into ADP releases mechanical energy in myosin motor heads. The internal energy that fuels this reaction can be written as the product of the average advancement of the reaction $\langle \xi_\mathrm{a} \rangle_\mathrm{b}$ and an affinity $\Delta\mu$, $\varphi_\mathrm{a} = -\Delta\mu \langle \xi_\mathrm{a} \rangle_\mathrm{b}$. Following [15], we consider that $\Delta\mu$ is maintained a constant throughout the process.

We now resort to an Onsager approach to determine the active flux $\underset{\sim}{\boldsymbol{j}}_\mathrm{a}$ specifying the power balance of the molecular motors,

$$\mathcal{D}_\mathrm{a} = \int_{\Omega(t)} \nu \left(\Delta\mu \langle \dot{\xi}_\mathrm{a} \rangle_\mathrm{b} - \kappa \langle \underset{\sim}{\boldsymbol{j}}_\mathrm{a} \cdot \underset{\sim}{\boldsymbol{r}} \rangle_\mathrm{b} \right) \mathrm{d}\boldsymbol{x}.$$

Since $\underset{\sim}{\boldsymbol{F}}_s = -\kappa \underset{\sim}{\boldsymbol{r}}$,

$$\Delta\mu \langle \dot{\xi}_\mathrm{a} \rangle_\mathrm{b} - \kappa \langle \underset{\sim}{\boldsymbol{j}}_\mathrm{a} \cdot \underset{\sim}{\boldsymbol{r}} \rangle_\mathrm{b} = \int_{\mathbb{R}^3} \left(\Delta\mu \dot{\xi}_\mathrm{a} + \underset{\sim}{\boldsymbol{F}}_s \cdot \underset{\sim}{\boldsymbol{j}}_\mathrm{a} \right) \psi_\mathrm{b} \, \mathrm{d}\boldsymbol{r},$$

making apparent the pairs of conjugate fluxes and forces $(\dot{\xi}_\mathrm{a},\ \Delta\mu)$ and $(\underset{\sim}{\boldsymbol{j}}_\mathrm{a},\ \underset{\sim}{\boldsymbol{F}}_s)$. In the same way as [33], we thus expand linearly the fluxes as:

$$\underset{\sim}{\boldsymbol{j}}_\mathrm{a} = \lambda_{11} \underset{\sim}{\boldsymbol{F}}_s + \underset{\sim}{\boldsymbol{\lambda}}_{12} \Delta\mu, \tag{11a}$$

$$\dot{\xi}_\mathrm{a} = \underset{\sim}{\boldsymbol{\lambda}}_{21} \cdot \underset{\sim}{\boldsymbol{F}}_s + \lambda_{22} \Delta\mu. \tag{11b}$$

The coefficient $\lambda_{11} \geq 0$ describes a slippage friction of the bound crosslinkers with respect to the polymer strand, which may constitute an additional source of relaxation of the network along with the unbinding–rebinding process. We can characterise it with a rate $\frac{1}{2} k_\mathrm{s}$ and a typical energy of the strands $\kappa\beta^{-2}$, yielding $\lambda_{11} = k_\mathrm{s}/(2\kappa)$. The other dissipative coefficient $\lambda_{22} \geq 0$ corresponds to the dissipation in the chemical reaction itself. As the dissipation $\mathcal{D}_a$ is positive,

$$\lambda_{22}\lambda_{11} \geq \underset{\sim}{\boldsymbol{\lambda}}_{21} \cdot \underset{\sim}{\boldsymbol{\lambda}}_{12}. \tag{12}$$

Following Onsager symmetry relations [34], we take equal reactive coefficients $\underset{\sim}{\boldsymbol{\lambda}}_{12} = \underset{\sim}{\boldsymbol{\lambda}}_{21}$. Since they are vectorial, a vector quantity has to be constructed at the microscale. One possibility is to use the strand vector $\underset{\sim}{\boldsymbol{r}}$ itself, which corresponds to the assumption that the orientation of $\underset{\sim}{\boldsymbol{r}}$ has a microscopic relevance. This is true for actin filaments, which are oriented, and myosin molecular motors which are able to sense this orientation. We call this the processive flux, use again $\kappa\beta^{-2}$ as the typical strand elastic energy to normalise the coefficients,

$$\underset{\sim}{\boldsymbol{\lambda}}_{12} = \frac{v_\mathrm{a}\beta^3}{\kappa} \theta(\boldsymbol{r}) \underset{\sim}{\boldsymbol{r}}, \qquad \underset{\sim}{\boldsymbol{j}}_\mathrm{a} = \left(\frac{v_\mathrm{a}\beta^3 \Delta\mu}{\kappa} \theta(\boldsymbol{r}) - \frac{1}{2} k_\mathrm{s} \right) \underset{\sim}{\boldsymbol{r}},$$

$$\dot{\xi}_\mathrm{a} = -v_\mathrm{a}\beta^3 \theta(\boldsymbol{r}) \boldsymbol{r}^2 + \lambda_{22} \Delta\mu,$$

where θ is some nondimensional function of $\underset{\sim}{\boldsymbol{r}}$ and we have introduced the velocity of processivity of motors v_a, which, in the absence of slippage, can be related to the rate of detachment k_u by the distance ℓ_a that motors travel along a strand before detaching, $\ell_\mathrm{a} = v_\mathrm{a}/k_\mathrm{u}$. If there is a nonzero slippage rate k_s, we can interpret a distance $\ell_\mathrm{a} = v_\mathrm{a}/(k_\mathrm{u} + k_\mathrm{s})$ in a

similar way. The specific energetic contribution of the flux $\underset{\sim}{\boldsymbol{j}}_{\mathrm{a}}$ can then be characterised as proportional to:

$$\langle \underset{\sim}{\boldsymbol{r}} \cdot \underset{\sim}{\boldsymbol{j}}_{\mathrm{a}} \rangle_{\mathrm{b}} = \frac{k_{\mathrm{u}} + k_{\mathrm{s}}}{2} \underset{\approx}{\mathbf{A}}_{\mathrm{a}} : \underset{\approx}{\mathbf{I}} - \frac{k_{\mathrm{s}}}{2} \underset{\approx}{\mathbf{A}} : \underset{\approx}{\mathbf{I}} \qquad \text{with} \qquad \underset{\approx}{\mathbf{A}}_{\mathrm{a}} = \frac{2\ell_{\mathrm{a}}\beta^3 \Delta\mu}{\kappa} \langle \theta(\boldsymbol{r}) \underset{\sim}{\boldsymbol{r}} \underset{\sim}{\boldsymbol{r}} \rangle_{\mathrm{b}}. \tag{13}$$

The slippage introduced by k_{s} thus results in a dissipation, whereas the first term is the trace of what we define as a *contractility tensor* $\underset{\approx}{\mathbf{A}}_{\mathrm{a}}$. We already define an associated *active stress tensor* $\underset{\approx}{\boldsymbol{\sigma}}_{\mathrm{a}} = \nu\kappa \underset{\approx}{\mathbf{A}}_{\mathrm{a}}$, which will be useful in Sect. 2.4.

One interesting case is to take $\theta(\underset{\sim}{\boldsymbol{r}}) = 1/(\beta \boldsymbol{r})^2$. Indeed, we then have

$$\underset{\sim}{\boldsymbol{j}}_{\mathrm{a}}^0 = (k_{\mathrm{u}} + k_{\mathrm{s}}) \ell_{\mathrm{a}} \frac{\beta \Delta\mu}{\kappa |\underset{\sim}{\boldsymbol{r}}|} \frac{\underset{\sim}{\boldsymbol{r}}}{|\underset{\sim}{\boldsymbol{r}}|}$$

where the motors follow the filament direction $\underset{\sim}{\boldsymbol{r}}/|\underset{\sim}{\boldsymbol{r}}|$ but proceed with a velocity that decreases hyperbolically with increasing strand tension $\kappa|\underset{\sim}{\boldsymbol{r}}|$. The microstructure contractility tensor and active stress that arise can then be explicited as:

$$\underset{\approx}{\mathbf{A}}_{\mathrm{a}} = \frac{2\ell_{\mathrm{a}}\beta\Delta\mu}{\kappa} \langle \underset{\approx}{\mathbf{Q}} \rangle_{\mathrm{b}}, \qquad\qquad \underset{\approx}{\boldsymbol{\sigma}}_{\mathrm{a}} = 2\nu\ell_{\mathrm{a}}\beta\Delta\mu \langle \underset{\approx}{\mathbf{Q}} \rangle_{\mathrm{b}}.$$

with $\langle \underset{\approx}{\mathbf{Q}} \rangle_{\mathrm{b}} = \langle \underset{\sim}{\boldsymbol{r}} \underset{\sim}{\boldsymbol{r}} / \boldsymbol{r}^2 \rangle_{\mathrm{b}}$ the orientation tensor of the network, and is seen, for this particular choice of θ, to be independent of how much the network is stretched. Note that the 'stalling' behaviour of the motors in $\underset{\sim}{\boldsymbol{j}}_{\mathrm{a}}^0$ does not explicitly appear at the macroscopic scale, and conversely we have shown previously that macroscopic stalling can be a collective effect which is only modulated by molecular-scale stalling [28]. At the microscopic level, the thermodynamic inequality (12) on λ_{22} implies that this choice of $\theta(\boldsymbol{r})$ is only valid if the network can be shown not to collapse, $|\boldsymbol{r}| \geq r_0 > 0$.

The total contribution of active terms to dissipation is:

$$\mathcal{D}_{\mathrm{a}} = \int_{\Omega(t)} \nu (k_{\mathrm{s}} \underset{\approx}{\mathbf{A}} : \underset{\approx}{\mathbf{I}} - 2 v_{\mathrm{a}} \beta^3 \Delta\mu + \lambda_{22} \Delta\mu^2) \, \mathrm{d}\boldsymbol{x}$$

and is positive under the condition that:

$$\lambda_{22} \geq \frac{2(k_{\mathrm{u}} + k_{\mathrm{s}})^2 \ell_{\mathrm{a}}^2}{k_{\mathrm{s}} k_B T} (2\pi\beta^{-1} \|\psi_{\mathrm{b}}\|_\infty + \beta^2) \geq \frac{2(k_{\mathrm{u}} + k_{\mathrm{s}})^2 \ell_{\mathrm{a}}^2}{k_{\mathrm{s}} k_B T} \left\langle \frac{1}{\boldsymbol{r}^2} \right\rangle_{\mathrm{b}}. \tag{14}$$

In what follows, we occasionally take the limit $k_{\mathrm{s}} \ll k_{\mathrm{u}}$ whereas k_{u} is close to the characteristic time of the processes of interest, implying that $(\ell_{\mathrm{a}}\beta)^2$ is small, limiting in turn the magnitude of $\underset{\approx}{\boldsymbol{\sigma}}_{\mathrm{a}}$. Note however that this is only for comparison with passive systems, since it simplifies the expression of factors, but it is in no way necessary.

Other choices are possible for the reactive coefficient $\underset{\sim}{\boldsymbol{\lambda}}_{12}$, see Appendix B. In particular, a model of "diffusive" flux along the filaments leads to the same form of the contractility tensor and active stress but a different prefactor. The orientation tensor $\langle \underset{\approx}{\mathbf{Q}} \rangle_{\mathrm{b}} = \langle \underset{\sim}{\boldsymbol{r}} \underset{\sim}{\boldsymbol{r}} / \boldsymbol{r}^2 \rangle_{\mathrm{b}}$ can be seen as a generalisation of the nematic tensor, in that it allows e.g. isotropy in a plane tangential to a surface.

Note that the velocity v_{a} and corresponding length ℓ_{a} can depend on the position in physical space, e.g. they may depend on the local concentration of some catalytic species.

2.4 Constitutive Equation of Active Networks

Having defined the stress tensor in Sect. 2.2, we can proceed with the usual procedure of bead–spring models in order to determine the constitutive equation that relates stress and strain, and which consists in multiplying the Smoluchowski Eq. (6) by the tensor $\underset{\sim}{\boldsymbol{r}}\underset{\sim}{\boldsymbol{r}}$ and integrating over the phase space. This yields:

$$\frac{\mathrm{d}\underset{\approx}{\mathbf{A}}}{\mathrm{d}t} - \underset{\approx}{\boldsymbol{\ell}} \cdot \underset{\approx}{\mathbf{A}} - \underset{\approx}{\mathbf{A}} \cdot \underset{\approx}{\boldsymbol{\ell}}^{\mathsf{T}} = -k_{\mathrm{u}} \int_{\mathbb{R}^3} \mathcal{K}_0(\psi_{\mathrm{b}}) \underset{\sim}{\boldsymbol{r}}\underset{\sim}{\boldsymbol{r}} \,\mathrm{d}\boldsymbol{r} + \langle \underset{\sim}{\boldsymbol{r}}\underset{\sim}{\boldsymbol{j}}_{\mathrm{a}} + \underset{\sim}{\boldsymbol{j}}_{\mathrm{a}}\underset{\sim}{\boldsymbol{r}} \rangle_{\mathrm{b}}, \tag{15}$$

where the tensor $\langle \underset{\sim}{\boldsymbol{r}}\underset{\sim}{\boldsymbol{j}}_{\mathrm{a}} + \underset{\sim}{\boldsymbol{j}}_{\mathrm{a}}\underset{\sim}{\boldsymbol{r}} \rangle_{\mathrm{b}}$ is the only new term compared to [26, p. 44]. From (13), we have $\langle \underset{\sim}{\boldsymbol{r}}\underset{\sim}{\boldsymbol{j}}_{\mathrm{a}} + \underset{\sim}{\boldsymbol{j}}_{\mathrm{a}}\underset{\sim}{\boldsymbol{r}} \rangle_{\mathrm{b}} = (k_{\mathrm{u}} + k_{\mathrm{s}})\underset{\approx}{\mathbf{A}}_{\mathrm{a}} - k_{\mathrm{s}}\underset{\approx}{\mathbf{A}}$.

We denote the upper-convected derivative of a tensor $\underset{\approx}{\mathbf{T}}$ by

$$\overset{\triangledown}{\underset{\approx}{\mathbf{T}}} = \frac{\mathrm{d}\underset{\approx}{\mathbf{T}}}{\mathrm{d}t} - \underset{\approx}{\boldsymbol{\ell}} \cdot \underset{\approx}{\mathbf{T}} - \underset{\approx}{\mathbf{T}} \cdot \underset{\approx}{\boldsymbol{\ell}}^{\mathsf{T}}, \tag{16}$$

The fact that this particular objective derivative arises is due to the contra-variant nature of the vector $\underset{\sim}{\boldsymbol{R}}$ which represents the fibrous microstructure [35]. It is thus not an arbitrary choice but an intrinsic property of materials formed of a network of entropic chains. Note also that the nonlinearity in Eq. (16) is not likely to be eliminated by an order of magnitude analysis: indeed, if the shear rate is of order $1/T$, then both the partial derivative in time and the velocity gradient $\underset{\approx}{\boldsymbol{\ell}}^{\mathsf{T}}$ are of order $1/T$. The legitimate linearisation of such a viscoelastic constitutive equation is thus a purely viscous constitutive equation.

Since we have chosen to assume constant rates of binding and unbinding, $\mathcal{K}_0 = \psi_{\mathrm{b}} - a_{\mathrm{u}}(k_{\mathrm{b}}/k_{\mathrm{u}})\psi_0$, we obtain that

$$-k_{\mathrm{u}} \int_{\mathbb{R}^3} \mathcal{K}_0(\psi_{\mathrm{b}}) \underset{\sim}{\boldsymbol{r}}\underset{\sim}{\boldsymbol{r}} \,\mathrm{d}\boldsymbol{r} = -k_{\mathrm{u}}\underset{\approx}{\mathbf{A}} + a_{\mathrm{u}}k_{\mathrm{b}}\beta^{-2}\underset{\approx}{\mathbf{I}}.$$

Altogether, this leads to:

$$\tau \overset{\triangledown}{\underset{\approx}{\mathbf{A}}} = \underset{\approx}{\mathbf{A}}_0 - \underset{\approx}{\mathbf{A}} + \underset{\approx}{\mathbf{A}}_{\mathrm{a}}, \tag{17}$$

where we have identified $\underset{\approx}{\mathbf{A}}_0 = a_{\mathrm{u}}k_{\mathrm{b}}/(k_{\mathrm{u}} + k_{\mathrm{s}}) \left\langle \underset{\sim}{\boldsymbol{r}}\underset{\sim}{\boldsymbol{r}} \right\rangle_0$ as the long-time limit of $\underset{\approx}{\mathbf{A}}$ in the absence of flow and activity, thus corresponding to relaxed chains. Comparing with Sect. 2.2 and since $\langle \underset{\sim}{\boldsymbol{r}}\underset{\sim}{\boldsymbol{r}} \rangle_0 = \frac{\beta^{-2}}{2}\underset{\approx}{\mathbf{I}}$, we set $a_0 = a_{\mathrm{u}}k_{\mathrm{b}}/(2k_{\mathrm{u}} + 2k_{\mathrm{s}}) \simeq \frac{1}{2}$ for $k_{\mathrm{s}} \ll k_{\mathrm{u}} \ll k_{\mathrm{b}}$. We have defined the *relaxation time* of the network as $\tau = (k_{\mathrm{u}} + k_{\mathrm{s}})^{-1}$, thus based on the average rate of the unbinding-rebinding process and of the internal slippage process.

We can also rewrite the specific free energy as the sum of the entropic energy of bound and unbound chains,

$$\varphi_{\mathrm{e}} = \frac{\kappa}{2} \int_{\mathbb{R}^3} (\psi_{\mathrm{b}} + \psi_{\mathrm{u}}) \boldsymbol{r}^2 \,\mathrm{d}\boldsymbol{r} = \frac{\kappa}{2} \operatorname{tr} \underset{\approx}{\mathbf{A}} + \frac{3}{2} a_{\mathrm{u}} k_B T.$$

Using the definition of $\underset{\approx}{\boldsymbol{\sigma}}$, and observing that $\overset{\triangledown}{\underset{\approx}{\mathbf{I}}} = -2\underset{\approx}{\boldsymbol{d}}$, we find:

$$\tau \overset{\triangledown}{\underset{\approx}{\boldsymbol{\sigma}}} + \underset{\approx}{\boldsymbol{\sigma}} = 2\tau G \underset{\approx}{\boldsymbol{d}} + \underset{\approx}{\boldsymbol{\sigma}}_{\mathrm{a}} \tag{18}$$

in the case when $\mu = 0$, which is the upper-convected Maxwell constitutive equation with relaxation time τ and short-time elastic modulus $G = \frac{k_{\mathrm{b}}}{k_{\mathrm{u}}} a_{\mathrm{u}} \nu k_B T \simeq \nu k_B T$ for $k_{\mathrm{u}} \ll k_{\mathrm{b}}$. The

Oldroyd-B model can be obtained with a nonzero liquid bath viscosity μ. There is a single relaxation time that appears in this model, which combines two relaxation processes of different nature (unbinding/rebinding k_u and internal slippage k_s). One could consider extensions to multiple relaxation modes in the spirit of the Lodge model [25, 36] or other models involving multiple crosslinks per chain [37]. If $\underset{\sim}{\boldsymbol{j}}_\mathrm{a}$ is nonzero, there is an additional term, $\underset{\approx}{\boldsymbol{\sigma}}_\mathrm{a} = \nu\kappa\underset{\approx}{\mathbf{A}}_\mathrm{a}$ that can be interpreted as a dynamic prestress [12] and can be identified with the active stress of the active gel theory [15].

2.5 Dissipation and Viscoelastic Relaxation

Using the definition of $\underset{\approx}{\mathbf{A}}$ and $\underset{\approx}{\mathbf{A}}_0$, we evaluate the part of the dissipation which is due to the unbinding–rebinding dynamics:

$$\mathcal{D}_\mathrm{r} = \frac{1}{2}\int_{\Omega(t)} k_\mathrm{u}\nu\kappa(\underset{\approx}{\mathbf{A}} - \underset{\approx}{\mathbf{A}}_0) : \underset{\approx}{\mathbf{I}}\,\mathrm{d}\boldsymbol{x}.$$

The term $-\frac{\nu\kappa}{2}\underset{\approx}{\mathbf{A}}_0 : \underset{\approx}{\mathbf{I}} = -\frac{3}{2}\nu k_B T$ for $k_\mathrm{s} \ll k_\mathrm{u} \ll k_\mathrm{b}$, corresponds to the thermal energy due to the equipartition of the unbound chains with the bath. It is thus a lower bound for the elastic energy $\nu\kappa\underset{\approx}{\mathbf{A}}$. See [38] and Appendix C for a proof that this is the case with $\underset{\approx}{\mathbf{A}}$ obeying (17) as long as the initial condition is admissible, $\det(\underset{\approx}{\mathbf{A}}(t=0)) \geq \det(\underset{\approx}{\mathbf{A}}_0)$, and only if the active stress is contractile, that is $\underset{\approx}{\mathbf{A}}_\mathrm{a}$ positive semi-definite.

Note that as seen in Sect. 2.3, the active crosslinkers are thermodynamically required to have a 'slippage' rate which has a dissipative trace of the form $\frac{1}{2}k_\mathrm{s}\nu\kappa\underset{\approx}{\mathbf{A}} : \underset{\approx}{\mathbf{I}}$ similar to the relaxation via unbinding, $\frac{1}{2}k_\mathrm{u}\nu\kappa\underset{\approx}{\mathbf{A}} : \underset{\approx}{\mathbf{I}}$. This combination gives the final relaxation time of the network $\tau = (k_\mathrm{u} + k_\mathrm{s})^{-1}$ in (17).

We can make use of the relaxation Eq. (17) to justify that $\mathcal{D}_\mathrm{r}$ corresponds to viscoelastic relaxation:

$$\mathcal{D}_\mathrm{r} = \frac{1}{2}\int_{\Omega(t)} \nu\kappa k_\mathrm{u}(-\tau\overset{\triangledown}{\underset{\approx}{\mathbf{A}}} + \underset{\approx}{\mathbf{A}}_\mathrm{a}) : \underset{\approx}{\mathbf{I}}\,\mathrm{d}\boldsymbol{x}.$$

Thus, in the passive viscoelastic case $\underset{\approx}{\mathbf{A}}_\mathrm{a} = \underset{\approx}{\mathbf{0}}$, the relaxation term is indeed proportional to the (negative) trace of $\overset{\triangledown}{\underset{\approx}{\mathbf{A}}}$ corresponding to the microstructure dissipating elastic energy. In the active case where $\underset{\approx}{\mathbf{A}}_\mathrm{a} \neq \underset{\approx}{\mathbf{0}}$ and is positive semi-definite, we still have $\mathcal{D}_\mathrm{r} \geq 0$, however the active strain is superimposed to the relaxation dynamics.

2.6 Summary

Here we take the limit $k_\mathrm{s} \ll k_\mathrm{u} \ll k_\mathrm{b}$, and hence $\tau = 1/k_\mathrm{u}$, and summarise the equations to obtain a closed model. The flow rate has to be such that $|\underset{\sim}{\nabla}\underset{\sim}{\boldsymbol{v}}| \lesssim k_\mathrm{b}$. The total specific free energy is then

$$\varphi = \varphi_\mathrm{e} + \varphi_\mathrm{a} = \frac{\kappa}{2}\,\mathrm{tr}\,\underset{\approx}{\mathbf{A}}(\boldsymbol{x},t) - \Delta\mu\langle\xi_\mathrm{a}\rangle_\mathrm{b}(\boldsymbol{x},t), \tag{19}$$

where $\kappa = 2k_B T\beta^2$. The thermodynamics of the system constrains the time evolution of the microstructure tensor $\underset{\approx}{\mathbf{A}}$, which relaxes towards a state that can be prestrained by molecular motors with the dynamics given in Eq. (17),

$$\tau\overset{\triangledown}{\underset{\approx}{\mathbf{A}}} = -\underset{\approx}{\mathbf{A}} + \underset{\approx}{\mathbf{A}}_0 + \underset{\approx}{\mathbf{A}}_\mathrm{a},$$

where the microstructure passive equilibrium tensor is $\underset{\approx}{\mathbf{A}}_0 = \frac{\beta^{-2}}{2}\underset{\approx}{\mathbf{I}}$. The contractility is $\underset{\approx}{\mathbf{A}}_\mathrm{a} = a_\mathrm{a}^2\langle\underset{\approx}{\mathbf{Q}}\rangle_\mathrm{b}$, where $a_\mathrm{a}^2 = 2\ell_\mathrm{a}\beta\Delta\mu/\kappa$ characterises the motor activity. The orientation tensor $\langle\underset{\approx}{\mathbf{Q}}\rangle_\mathrm{b} = \langle\underset{\sim}{\boldsymbol{r}}\underset{\sim}{\boldsymbol{r}}/\boldsymbol{r}^2\rangle_\mathrm{b}$ is not equal to the microstructure tensor $\underset{\approx}{\mathbf{A}} = \langle\underset{\sim}{\boldsymbol{r}}\underset{\sim}{\boldsymbol{r}}\rangle_\mathrm{b}$. It can in some cases be deduced from the symmetries of the flow, see Sect. 4 and e.g. [39]. It is also sometimes assumed to be isotropic. It could also be approximated to $\underset{\approx}{\mathbf{A}}/(\underset{\approx}{\mathbf{A}} : \underset{\approx}{\mathbf{I}})$, or finally could be calculated using a multiscale model that would solve Eq. (6) explicitely [40].

The density of chains evolves with

$$\frac{\partial \nu}{\partial t} + \underset{\sim}{\nabla}\cdot(\nu\underset{\sim}{\boldsymbol{v}}) = 0. \tag{20}$$

The total stress tensor is $-p\underset{\approx}{\mathbf{I}} + \underset{\approx}{\boldsymbol{\sigma}}$, where the extra stress $\underset{\approx}{\boldsymbol{\sigma}}$ originates from the network configuration and from possible viscous contributions,

$$\underset{\approx}{\boldsymbol{\sigma}} = \nu\kappa(\underset{\approx}{\mathbf{A}} - \underset{\approx}{\mathbf{A}}_0) + 2\mu\underset{\approx}{\boldsymbol{d}}, \tag{21a}$$

and the pressure p is the Lagrange multiplier that ensures

$$\underset{\sim}{\nabla}\cdot\underset{\sim}{\boldsymbol{v}} = 0. \tag{21b}$$

Initial conditions are required for ν and $\underset{\approx}{\mathbf{A}}$. The momentum balance and associated boundary conditions are given in Eqs. (7a) and (7b), which allows to solve for the velocity $\underset{\sim}{\boldsymbol{v}}$.

The present model Eqs. (17), (21a)–(21b), (7a)–(7b), (20) can thus be solved for the time evolution of the microstructure tensor $\underset{\approx}{\mathbf{A}}$ and extra stress tensor $\underset{\approx}{\boldsymbol{\sigma}}$ and pressure p, network velocity $\underset{\sim}{\boldsymbol{v}}$ and density ν. Note that Eqs. (17), (21a)–(21b) can be combined to eliminate the microstructure tensor $\underset{\approx}{\mathbf{A}}$ and solve directly in terms of the extra stress $\underset{\approx}{\boldsymbol{\sigma}}$, giving Eq. (18).

When the characteristic time of the flow is very long compared to the relaxation time τ, a viscous limit of Eq. (18) eliminating $\tau\overset{\triangledown}{\underset{\approx}{\boldsymbol{\sigma}}}$ but retaining the anisotropic active stress $\underset{\approx}{\boldsymbol{\sigma}}_\mathrm{a}$ can be taken, this is the model used e.g. in [39]. Otherwise, the nonlinear objective derivative $\overset{\triangledown}{\underset{\approx}{\boldsymbol{\sigma}}} = \mathrm{d}\underset{\approx}{\boldsymbol{\sigma}}/\mathrm{d}t - (\underset{\sim}{\nabla}\underset{\sim}{\boldsymbol{v}})^\mathsf{T}\underset{\approx}{\boldsymbol{\sigma}} - \underset{\approx}{\boldsymbol{\sigma}}\underset{\sim}{\nabla}\underset{\sim}{\boldsymbol{v}}$ is required in order to account for the entropic nature of the microstructure. This is the case even when the problem can be reduced to a one-dimensional case ($\underset{\approx}{\boldsymbol{\sigma}} = \sigma_{xx}\underset{\sim}{\boldsymbol{e}}_x\underset{\sim}{\boldsymbol{e}}_x$, $\underset{\sim}{\boldsymbol{v}} = v_x\underset{\sim}{\boldsymbol{e}}_x$) [28, 41] since, contrarily to the co-rotational objective derivative [42], a nonlinear coupling remains in the longitudinal component $(\overset{\triangledown}{\underset{\approx}{\boldsymbol{\sigma}}})_{xx} = \mathrm{d}\sigma_{xx}/\mathrm{d}t - 2(\partial_x v_x)\sigma_{xx}$. Taking values from e.g. recoil after laser ablation of actomyosin experiments [43], one can estimate that the order of magnitude of this nonlinear term is similar or larger than the viscous one. This could provide an alternative way to test experimentally whether a biopolymer network exhibits entropic or enthalpic elasticity.

3 Multiplicative Strain Decomposition Framework

Multiplicative decomposition of the deformation gradient is commonly used for thermoelasticity and elastoplasticity applications [44]. It has also proven very useful in biomechanics, where the main applications have been the understanding of residual stress originating from growth in soft tissue [1, 45] but also plants or hard tissue [46]. In these contexts, growth is then considered as a prestrain. Prestrain can also be used to model contractility, as e.g. in [47], and indeed there exist formal analogies [12].

For liquid-like systems, an additional phenomenon is the microstructure relaxation. Many numerical models that aim at reproducing the phenomenology of microstructure relaxation use an algorithm that can formally be likened to morphoelasticity: at each time step, solve

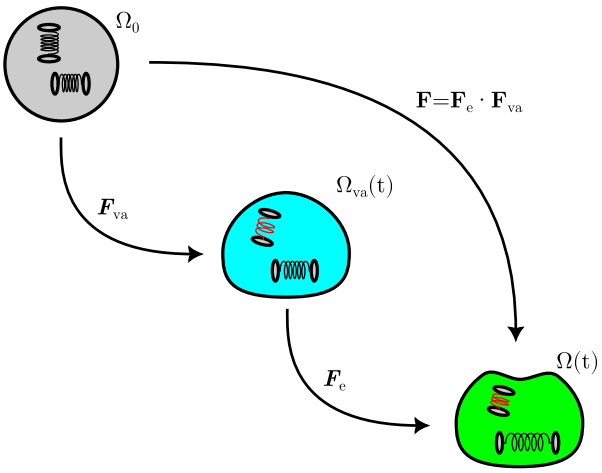

Fig. 2 Multiplicative decomposition of the deformation gradient for viscoelastic active fluids

for the elastic deformation relative to some intermediate configuration, this configuration being the equilibrium configuration of the previous time step. Formally, this corresponds to a morphoelastic model where the anelastic defomations are the viscous-like deformations cumulated through time. This is extremely convenient for e.g. the dynamics of slender liquid visco-elastic structures [48, 49]. However this approach is very crude in the sense that it cannot describe any dynamics at a characteristic time close or smaller than the relaxation time of the material, and of course that its thermodynamics are uncontrolled. Recently, a multiplicative strain decomposition has been introduced [50] for viscoelatic liquid models.

Here, we make use of the multiplicative decomposition of the deformation gradient formalism and derive the evolution equation of the anelastic part of the deformation so that it matches the active viscoelastic model developed in the previous section.

We choose the decomposition as $\underset{\approx}{\mathbf{F}} = \underset{\approx}{\mathbf{F}}_e \cdot \underset{\approx}{\mathbf{F}}_{va}$, illustrated in Fig. 2, where $\underset{\approx}{\mathbf{F}}_e$ corresponds to elastic deformations of the microstructure, and $\underset{\approx}{\mathbf{F}}_{va}$ corresponds to both viscous-like deformations due to the relaxation of the elastic microstructure and active deformation due to a chemically-driven growth or contraction of the microstructure. Our objective is to obtain a set of equations equivalent to the model of Sect. 2.6 in terms of $(\underset{\approx}{\mathbf{F}}_{va}, \underset{\approx}{\mathbf{F}}_e, p)$.

The tensor $\underset{\approx}{\mathbf{A}}$ is by construction symmetric and positive semidefinite (and positive definite as long as Supp ψ_b has nonzero measure, which can be ensured by smooth initial conditions and the affine or diffusive nature of the fluxes in Eq. (6)). Thus Cholesky factorisation guarantees the existence of an upper triangular tensor $\underset{\approx}{\mathbf{U}}$ such that $\underset{\approx}{\mathbf{A}} = \underset{\approx}{\mathbf{U}}^{\mathsf{T}} \cdot \underset{\approx}{\mathbf{U}}$. Thus we can define $\underset{\approx}{\mathbf{F}}_e$ so that $\underset{\approx}{\mathbf{A}}$ is either $\alpha \underset{\approx}{\mathbf{F}}_e^{\mathsf{T}} \cdot \underset{\approx}{\mathbf{F}}_e$ or $\alpha \underset{\approx}{\mathbf{F}}_e \cdot \underset{\approx}{\mathbf{F}}_e^{\mathsf{T}}$, with α a constant, imposing that the upper diagonal matrix in the QR-decomposition of $\underset{\approx}{\mathbf{F}}_e$ is $\underset{\approx}{\mathbf{U}}$. Since in both choices, the invariants $\underset{\approx}{\mathbf{F}}_e^{\mathsf{T}} \cdot \underset{\approx}{\mathbf{F}}_e : \underset{\approx}{\mathbf{I}} = \underset{\approx}{\mathbf{F}}_e \cdot \underset{\approx}{\mathbf{F}}_e^{\mathsf{T}} : \underset{\approx}{\mathbf{I}} = \underset{\approx}{\mathbf{F}}_e : \underset{\approx}{\mathbf{F}}_e$ are identical, we make our choice in order to be able to define the corresponding $\underset{\approx}{\mathbf{F}}_{va}$ conveniently. As in [51], we remark that the (Eulerian) *left* Cauchy–Green tensor $\underset{\approx}{\mathbf{B}} = \underset{\approx}{\mathbf{F}} \cdot \underset{\approx}{\mathbf{F}}^{\mathsf{T}}$ is such that $\dot{\underset{\approx}{\mathbf{B}}} = \underset{\approx}{\boldsymbol{\ell}} \cdot \underset{\approx}{\mathbf{B}} + \underset{\approx}{\mathbf{B}} \cdot \underset{\approx}{\boldsymbol{\ell}}^{\mathsf{T}}$ and thus, that its upper convected derivative is zero, which guides us to choose $\underset{\approx}{\mathbf{F}}_e$ such that $\underset{\approx}{\mathbf{F}}_e \cdot \underset{\approx}{\mathbf{F}}_e^{\mathsf{T}} = \alpha \underset{\approx}{\mathbf{A}}$.

As a result, $\underset{\approx}{\mathbf{A}} = \alpha^{-1} \underset{\approx}{\mathbf{F}} \cdot \underset{\approx}{\mathbf{C}}_{va}^{-1} \cdot \underset{\approx}{\mathbf{F}}^{\mathsf{T}}$ with $\underset{\approx}{\mathbf{C}}_{va}^{-1} = \underset{\approx}{\mathbf{F}}_{va}^{-1} \cdot \underset{\approx}{\mathbf{F}}_{va}^{-\mathsf{T}}$, and by derivation

$$\overset{\triangledown}{\underset{\approx}{\mathbf{A}}} = \dot{\underset{\approx}{\mathbf{A}}} - \underset{\approx}{\boldsymbol{\ell}} \cdot \underset{\approx}{\mathbf{A}} - \underset{\approx}{\mathbf{A}} \cdot \underset{\approx}{\boldsymbol{\ell}}^{\mathsf{T}} = \alpha^{-1} \underset{\approx}{\mathbf{F}} \cdot \frac{\mathrm{d}\underset{\approx}{\mathbf{C}}_{va}^{-1}}{\mathrm{d}t} \cdot \underset{\approx}{\mathbf{F}}^{\mathsf{T}}$$

which allows to use Eq. (17) to set the dynamics of $\underset{\approx}{\mathbf{C}}_{\mathrm{va}}^{-1}$,

$$\tau \underset{\approx}{\mathbf{F}} \cdot \frac{\mathrm{d}\underset{\approx}{\mathbf{C}}_{\mathrm{va}}^{-1}}{\mathrm{d}t} \cdot \underset{\approx}{\mathbf{F}}^{\mathsf{T}} = -\underset{\approx}{\mathbf{F}} \cdot \underset{\approx}{\mathbf{C}}_{\mathrm{va}}^{-1} \cdot \underset{\approx}{\mathbf{F}}^{\mathsf{T}} + \alpha \underset{\approx}{\mathbf{A}}_0 + \alpha \underset{\approx}{\mathbf{A}}_{\mathrm{a}}$$

which yields, since $\underset{\approx}{\mathbf{A}}_0 = a_0 \beta^{-2} \underset{\approx}{\mathbf{I}}$,

$$\tau \frac{\mathrm{d}\underset{\approx}{\mathbf{C}}_{\mathrm{va}}^{-1}}{\mathrm{d}t} = -\underset{\approx}{\mathbf{C}}_{\mathrm{va}}^{-1} + \alpha a_0 \underset{\approx}{\mathbf{C}}^{-1} + \alpha \underset{\approx}{\mathbf{F}}^{-1} \cdot \underset{\approx}{\mathbf{A}}_{\mathrm{a}} \cdot \underset{\approx}{\mathbf{F}}^{-\mathsf{T}}. \tag{22}$$

where α remains to be determined. In the permanent regime and in the absence of activity $\underset{\approx}{\mathbf{A}}_{\mathrm{a}}$, elastic strains relax and thus $\underset{\approx}{\mathbf{C}}_{\mathrm{va}}^{-1}$ tends to $\underset{\approx}{\mathbf{C}}^{-1}$. We thus set $\alpha = \beta^2 a_0^{-1}$ using this limit behaviour. For $k_{\mathrm{b}} \gg k_{\mathrm{u}}$, this is thus $\alpha = 2\beta^2$. For convenience, we define the *active strain tensor* $\underset{\approx}{\mathbf{E}}_{\mathrm{a}} = -\alpha \underset{\approx}{\mathbf{A}}_{\mathrm{a}}$. Since our theory requires that $\underset{\approx}{\mathbf{A}}_{\mathrm{a}}$ is positive semi-definite (Appendix C), $\underset{\approx}{\mathbf{E}}_{\mathrm{a}}$ is negative. Thus, the active stress $\underset{\approx}{\boldsymbol{\sigma}}_{\mathrm{a}}$ defined in Sect. 2.4 is $\underset{\approx}{\boldsymbol{\sigma}}_{\mathrm{a}} = -G \underset{\approx}{\mathbf{E}}_{\mathrm{a}}$. Note that our model of active crosslinkers leads to nonpositive eigenvalues of $\underset{\approx}{\mathbf{E}}_{\mathrm{a}}$ (interpreted as a contractile, thus negative, prestrain) and hence nonnegative ones of $\underset{\approx}{\boldsymbol{\sigma}}_{\mathrm{a}}$.

In summary, the model of Sect. 2.6 can now be rewritten using the multiplicative decomposition. Given $\underset{\approx}{\mathbf{E}}_{\mathrm{a}}$, G, μ, τ, find $(\underset{\approx}{\mathbf{C}}_{\mathrm{va}}, \underset{\sim}{\boldsymbol{u}}, p)$ such that:

$$\tau \frac{\mathrm{d}\underset{\approx}{\mathbf{C}}_{\mathrm{va}}^{-1}}{\mathrm{d}t} = -\underset{\approx}{\mathbf{C}}_{\mathrm{va}}^{-1} + \underset{\approx}{\mathbf{F}}^{-1} \cdot (\underset{\approx}{\mathbf{I}} - \underset{\approx}{\mathbf{E}}_{\mathrm{a}}) \cdot \underset{\approx}{\mathbf{F}}^{-\mathsf{T}}, \tag{23a}$$

$$\underset{\sim}{\nabla} \cdot \underset{\approx}{\boldsymbol{\sigma}}[\underset{\approx}{\mathbf{C}}_{\mathrm{va}}^{-1}, \underset{\sim}{\boldsymbol{u}}] - \underset{\sim}{\nabla} p = \underset{\sim}{\mathbf{0}}, \tag{23b}$$

$$\det \underset{\approx}{\mathbf{F}}[\underset{\sim}{\boldsymbol{u}}] = 1, \tag{23c}$$

where

$$\underset{\approx}{\boldsymbol{\sigma}} = G(\underset{\approx}{\mathbf{B}}_{\mathrm{e}}[\underset{\sim}{\boldsymbol{u}}] - \underset{\approx}{\mathbf{I}}) + \mu(\underset{\approx}{\boldsymbol{\ell}} + \underset{\approx}{\boldsymbol{\ell}}^{\mathsf{T}}), \tag{23d}$$

$$\underset{\approx}{\mathbf{F}} = \underset{\approx}{\mathbf{I}} + \underset{\sim}{\nabla} \underset{\sim}{\boldsymbol{u}}^{\mathsf{T}}, \qquad \underset{\approx}{\mathbf{B}}_{\mathrm{e}} = \underset{\approx}{\mathbf{F}} \cdot \underset{\approx}{\mathbf{C}}_{\mathrm{va}}^{-1} \cdot \underset{\approx}{\mathbf{F}}^{\mathsf{T}}, \qquad \underset{\approx}{\boldsymbol{\ell}} = \dot{\underset{\approx}{\mathbf{F}}} \cdot \underset{\approx}{\mathbf{F}}^{-1}, \tag{23e}$$

subject to an initial condition on $\underset{\approx}{\mathbf{C}}_{\mathrm{va}}$ and boundary conditions on $(\underset{\approx}{\boldsymbol{\sigma}} - p\underset{\approx}{\mathbf{I}}) \cdot \underset{\sim}{\boldsymbol{n}}$. As discussed above, if $\underset{\approx}{\mathbf{F}}_{\mathrm{va}}$ and $\underset{\approx}{\mathbf{F}}_{\mathrm{e}}$ are needed, then it has to be noted that any local rotation $\underset{\approx}{\mathbf{Q}}(\boldsymbol{x})$ of the intermediate configuration is permitted, since for $\underset{\approx}{\mathbf{Q}}$ an orthogonal matrix, $\underset{\approx}{\mathbf{F}}'_{\mathrm{e}} = \underset{\approx}{\mathbf{F}}_{\mathrm{e}} \cdot \underset{\approx}{\mathbf{Q}}$ and $\underset{\approx}{\mathbf{F}}'_{\mathrm{va}} = \underset{\approx}{\mathbf{Q}}^{\mathsf{T}} \cdot \underset{\approx}{\mathbf{F}}_{\mathrm{va}}$ are also solutions of the problem with unchanged $\underset{\approx}{\mathbf{F}}$, $\underset{\approx}{\mathbf{B}}_{\mathrm{e}}$, $\underset{\approx}{\mathbf{C}}_{\mathrm{va}}$. To fix this, one can e.g. impose that $\underset{\approx}{\mathbf{F}}_{\mathrm{e}}^{\mathsf{T}}$ is upper-triangular with positive diagonal coefficients.

4 Example Applications

We present here two examples in which the dynamics of an actively contractile structure can be solved in a straightforward manner thanks to the multiplicative decomposition of the deformation gradient. Anisotropic geometry and anisotropic contractility is present in both examples, either in aligned or orthogonal configurations. In both examples we neglect the liquid bath viscosity μ and take the orientation tensor $\langle \underset{\approx}{\mathbf{Q}} \rangle_{\mathrm{b}}$ as a given input.

4.1 Actin Stress Fibres: An Active Viscoelastic Beam in an Elastic Environment

We model a slender active viscoelastic beam, which can for example represent a stress fibre in a cell with adhesion at its ends only [52]. It initially spans the distance from $(-L_0, 0, 0)^\mathsf{T}$ to $(L_0, 0, 0)^\mathsf{T}$ and has radius r_0.

We assume that the chains within the beam are all oriented along the main axis x of the beam, leading to $\langle \underset{\approx}{\mathbf{Q}} \rangle_\mathrm{b} = \underset{\sim}{\boldsymbol{e}}_x \underset{\sim}{\boldsymbol{e}}_x$ and $\underset{\approx}{\mathbf{E}}_\mathrm{a} = -a^2 \underset{\sim}{\boldsymbol{e}}_x \underset{\sim}{\boldsymbol{e}}_x$. The external forces are supposed to be zero along the beam itself (no friction), except for tractions $\pm F \underset{\sim}{\boldsymbol{e}}_x = \pm k_s L_0 (1 - \lambda_x) \underset{\sim}{\boldsymbol{e}}_x$ applied at each end $x = \pm L_0$ of the beam and which correspond to the elastic resistance to the deformation of the environment which behaves as a spring of stiffness k_s. We define $E_s = k_s L_0 / (\pi r_0^2)$.

With this geometry and restricting load to the longitudinal direction only, the deformation gradient and stress tensors are diagonal tensors, $\underset{\approx}{\mathbf{F}} = \mathbf{diag}(\lambda_x, \lambda_r, \lambda_r)$ and $G(\underset{\approx}{\mathbf{F}}_\mathrm{e} \cdot \underset{\approx}{\mathbf{F}}_\mathrm{e}^\mathsf{T} - \underset{\approx}{\mathbf{I}}) = \mathbf{diag}(\sigma_{xx}, \sigma_{rr}, \sigma_{rr})$. Thus $\underset{\approx}{\mathbf{F}}_\mathrm{e} \cdot \underset{\approx}{\mathbf{F}}_\mathrm{e}^\mathsf{T}$ is diagonal, and we can choose $\underset{\approx}{\mathbf{F}}_\mathrm{e} = \mathbf{diag}(\alpha_x, \alpha_r, \alpha_r)$, $\underset{\approx}{\mathbf{F}}_\mathrm{va} = \mathbf{diag}(\gamma_x, \gamma_r, \gamma_r)$. By definition, $\lambda_i = \alpha_i \gamma_i$, $i \in \{r, x\}$.

We have the equilibrium equations:

$$G(\alpha_x^2 - 1) - p = E_s (1 - \lambda_x) \lambda_r^{-2} \tag{24}$$

$$G(\alpha_r^2 - 1) - p = 0 \tag{25}$$

$$\lambda_r^2 \lambda_x = 1 \tag{26}$$

Thus, subtracting the r equation from the x one to eliminate pressure, and using the incompressibility condition,

$$\lambda_x^2 - \lambda_x + \frac{G}{E_s} (\alpha_x^2 - \alpha_r^2) = 0.$$

From Eq. (23a), we have:

$$2\tau \dot{\gamma}_x = (\alpha_x^2 - 1 - a^2) \alpha_x^{-2} \gamma_x \tag{27}$$

$$2\tau \dot{\gamma}_r = (\alpha_r^2 - 1) \alpha_r^{-2} \gamma_r \tag{28}$$

For $a \leq a_c = \sqrt{E_s/(4G)}$, there is an admissible long times solution with $\alpha_x^2 = 1 + a^2$, $\alpha_r = 1$, for which $\gamma_i > 0$ and leading to $\lambda_x = \frac{1}{2}(1 + \sqrt{1 - 4Ga^2/E_s})$. See Fig. 3**B,C** for the dynamics leading to that asymptotic state. For $a > a_c$, the beam reaches length $L_0/2$ in finite time, which (provided that $\langle \underset{\approx}{\mathbf{Q}} \rangle_\mathrm{b}$ is unchanged) leads to a catastrophic collapse: indeed, the broadening section of the beam then dominates over its shortening, and the external traction (per unit surface of the section) then decreases with increasing deformation. The external traction is thus unable to balance the internal contractile stress for any deformation and the material flows towards a zero length of the "beam".

The relevance of this model for actomyosin-based systems is discussed in [28], where we also find that a viscoelastic liquid material with an internal active stress adapts in length to the external stiffness E_s. It may also be seen as a modelling framework for the so-called actin ventral stress fibres [53, 54].

4.2 Apical Luminal Surface: Actively Contractile Spherical Shell

Next, we turn to a 3D case where contractility is tangential to the surface of the structure. This can be inspired e.g. by the apical surfaces of cells organised as a spherical monolayer

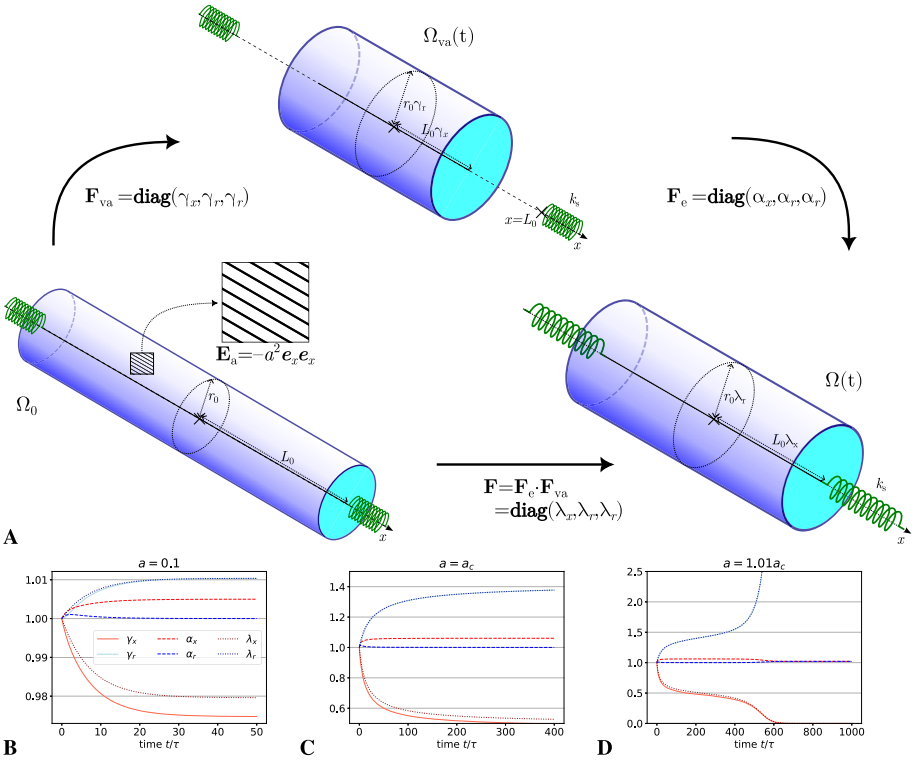

Fig. 3 Uniaxially contractile beam interacting with an elastic environment. **A**, The initial configuration Ω_0 of the beam, before the active strain $\underset{\approx}{\mathbf{E}}_a$ has been applied, is chosen here at equilibrium with the external springs. The visco-active deformation $\underset{\approx}{\mathbf{F}}_{va}(t)$ gives the intermediate virtual configuration $\Omega_{va}(t)$, a configuration which is not compatible with the external forces and does not obey incompressibility. The elastic deformation $\underset{\approx}{\mathbf{F}}_e(t)$ restores both of these requirements in the current configuration $\Omega(t)$. The time evolution of $\underset{\approx}{\mathbf{F}}_{va}(t)$ is prescribed by the relaxation dynamics of the microstructure $\underset{\approx}{\mathbf{A}}$ towards a state where the elastic stress is equal to the active stress, $\underset{\approx}{\boldsymbol{\sigma}}(t_{eq})=\nu\kappa(\underset{\approx}{\mathbf{A}}(t_{eq})-\underset{\approx}{\mathbf{A}}_0)=-G\underset{\approx}{\mathbf{E}}_a$. **B-D**, Dynamics for a contractile strain $\underset{\approx}{\mathbf{E}}_a=-a^2\underset{\sim}{\boldsymbol{e}}_x\underset{\sim}{\boldsymbol{e}}_x$ for different values of a and $G/E_s=1$. In all cases, the contractile strain drives an initial decreasing γ_x (active shortening) which is partly balanced by an increasing α_x (elastic stretch), resulting in a lesser shortening of the current configuration λ_x. Incompressibility imposes a swelling in the radial direction, $\lambda_r>1$, which after a transient elastic stretch $\alpha_r>1$ drives a viscoelastic relaxation towards $\gamma_r=\lambda_r$. **B**, for $a=0.1$, the contraction is 90% of the final contraction at $t\approx 17\tau$. **C**, for a equal to the critical value $a_c\approx 0.35$, the contraction is 90% of the final contraction at $t\approx 195\tau$. **D**, for a contractility slightly above the critical value, the contraction reaches the critical value 0.5 at $t\approx 229\tau$, the beam then collapses tending to 0 length while the radial stretch diverges

around a central lumen in a cyst [55], which can be represented by a thin, closed surface in elastic interaction with a spherically shaped basement membrane that contains it. For simplicity we will treat this surface as perfectly permeable, in reality the water flux itself is under an active control.

Figure 4 illustrates this spherical shell geometry, with initial outer radius $\rho(t=0)=\rho_0$ and finite thickness $h(t=0)=h_0\ll\rho_0$. We assume that it contracts tangentially in an isotropic manner and consider only solutions retaining spherical symmetry. Their stability will be studied elsewhere. Thus, $\underset{\approx}{\mathbf{E}}_a=-\frac{1}{2}a^2(\underset{\approx}{\mathbf{I}}-\underset{\sim}{\boldsymbol{e}}_r\underset{\sim}{\boldsymbol{e}}_r)$. The elastic interaction with a fixed outer sphere of radius ρ_0 is modelled by a Winkler elastic foundation characterised by a

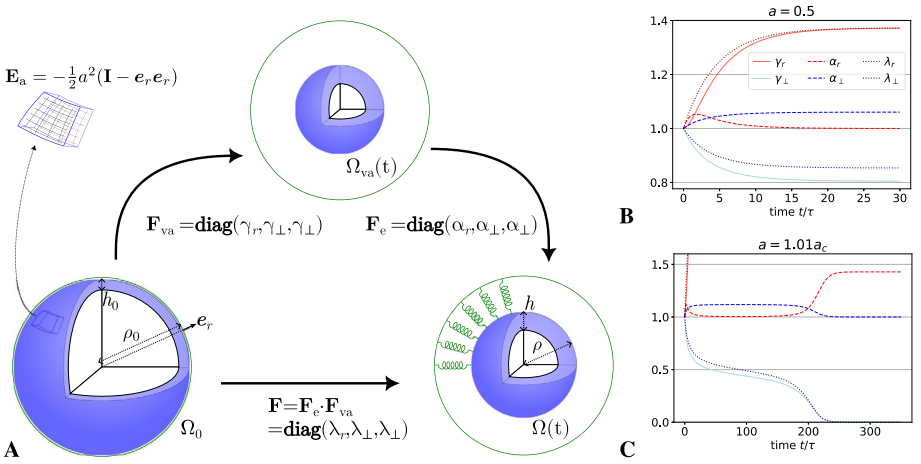

Fig. 4 Tangentially contractile sphere bound elastically to a fixed sphere. **A**, The initial, intermediate and current configurations of the contractile sphere. In the current configuration, mechanical balance with the Winkler foundation which binds it to a fixed sphere of radius ρ_0 has to be verified. **B,C**, Dynamics for $a_c = \sqrt{2}/2$ and an orthoradial contractile strain $\underset{\approx}{\mathbf{E}}_a = -\frac{1}{2}a^2(\underset{\approx}{\mathbf{I}} - \underset{\sim}{\boldsymbol{e}_r}\underset{\sim}{\boldsymbol{e}_r})$ with two different magnitudes of a, respectively below and above the critical value a_c. Transient behaviours similar to the case of the contractile beam are observed, although the axes in which they appear differs due to the different geometry and active stress orientation

spring stiffness k_s and a density Σ_0 on the outer sphere, and thus $\Sigma_s = \Sigma_0(\rho_0/\rho)^2$ on the outer surface of the shell. The boundary conditions are thus,

$$\underset{\approx}{\boldsymbol{\tau}}(\rho)\cdot\underset{\sim}{\boldsymbol{e}_r} = f_{\text{ext}}\underset{\sim}{\boldsymbol{e}_r} = E_s\frac{\rho_0(\rho_0-\rho)}{\rho^2}\underset{\sim}{\boldsymbol{e}_r}, \qquad \underset{\approx}{\boldsymbol{\tau}}(\rho-h)\cdot\underset{\sim}{\boldsymbol{e}_r} = \underset{\sim}{\mathbf{0}},$$

with $E_s = \Sigma_0\rho_0 k_s$. Spherical symmetry imposes that $\underset{\approx}{\boldsymbol{\tau}}$ and $\underset{\approx}{\mathbf{F}} = \mathbf{diag}(\lambda_r,\lambda_\perp,\lambda_\perp)$ are diagonal tensors. Hence, the current configuration is a spherical shell of outer surface area $4\pi(\lambda_\perp\rho_0)^2$, and thus radius $\rho = \rho_0\lambda_\perp$ and thickness $h = h_0\lambda_r = h_0/\lambda_\perp^2$. From (23d) and $\underset{\approx}{\mathbf{F}}_e$ being chosen upper diagonal, it must have the form $\underset{\approx}{\mathbf{F}}_e = \mathbf{diag}(\alpha_r,\alpha_\perp,\alpha_\perp)$ and hence $\underset{\approx}{\mathbf{F}}_{va} = \mathbf{diag}(\gamma_r,\gamma_\perp,\gamma_\perp)$.

For small h_0, we expand $\tau_{rr} = f_{\text{ext}}(r-\rho+h)/h + O(h_0^2)$ and the mechanical balance along the radial direction gives:

$$0 = [\underset{\sim}{\nabla}\cdot\underset{\approx}{\boldsymbol{\tau}}]_r = \frac{f_{\text{ext}}}{h} - \frac{2G}{r}(\alpha_\perp^2 - 1)$$

which results in an algebraic equation linking $\alpha_\perp$ and $\lambda_\perp$. As above, (23a) gives evolution equations for $(\gamma_r,\gamma_\perp)$ which allow to solve the dynamics (see Fig. 4B) and find a nondegenerate steady state for $a^2 \le a_c^2 = 4h_0G/(\rho_0E_s)$,

$$\alpha_\perp = \sqrt{1+\frac{a^2}{2}}, \quad \alpha_r = 1, \quad \lambda_\perp = \frac{1}{2}\left(1+\sqrt{1-\frac{a^2}{a_c^2}}\right), \quad \lambda_r = 1/\lambda_\perp^2.$$

For $a > a_c$, the shell collapses (Fig. 4C). Qualitatively, we obtain analogous phenomena as in the above case of the active beam, with a rich dynamical behaviour which can be solved in a convenient way thanks to the deformation gradient decomposition.

5 Conclusions

In this paper, we derive the specific shape and dependences on microscopic processes of active terms that are present in linearisations of the active gel theory [15] while ensuring that they are consistent with thermodynamical requirements. Rather than start from the free energy of nematic liquid crystals [15, 56], where no stretching of the microstructure is possible, we start from the entropic elasticity of Gaussian chains that model the actin filaments between two crosslinks. This possibility of stretching the filaments is at the origin of the specific shape of the objective derivative in the constitutive equation [35], whose nonlinearities are negligible only in the purely viscous limit. Thus, whenever the timescale of the process at play is comparable to the relaxation time, the correct form of the constitutive equation is an upper-convected viscoelastic liquid material law. The model we derive here has a single relaxation time, however similar extensions as those of the Lodge network model [27, p. 120] can be relevant for biopolymers [37], and could allow to fit the fractional exponents observed in experiments [57, 58]. The simplest of these laws, when only one relaxation time is present—either due to the material itself or because the timescale of the process is comparable but larger than the largest relaxation time—is the upper-convected Maxwell equation.

A link is explicitely made between the microscopic scale behaviour of molecular motors and the continuum scale active stress. Compared to a previous such attempt [28], we are now able to define conditions for which microscopic scale kinetics are thermodynamically admissible. When motors are assumed to walk randomly along actin filaments, we recapitulate the results from [28], reaching an anisotropic contractility which scales as the square of the length of the typical step performed by a power-stroke of the myosin. We can also envision a case where motors walk processively along polar filaments. The resulting shape of the anisotropic contractility remains similar as in the above case, but with a linear dependence in the step size and thus a higher efficiency. We show that this active contribution appears as an offset of the isotropic rest configuration of the microstructure to a new configuration with prestrained microstucture configuration.

Active biopolymer networks encompass both subcellular structures such as the actomyosin and, at a larger scale, fibrous tissue [12]. Contractility of actomyosin is also felt in cellularised tissue like epithelia [12, 59] which are often simulated with similar continuum models [39, 60]. For those it is not appropriate to use elastic chains as the microstructure, however when considering the kinetics of cell deformation and neighbour exchanges, models of the same shape as the present model are found, including the upper-convected objective derivative [61–63]. A possible direction for these materials is to consider a non-Hookean elasticity of the microstructure, e.g. with a finite extensibility approach [27, p. 142].

Viscoelastic liquids lead to mathematical problems notoriously difficult to solve analytically or numerically, and the set of equations in Sect. 2.6 can prove challenging to solve for complex geometries. In addition, biopolymer networks such as actomyosin often form thin shell-like structures [12], which turns the problem into a moving domain partial differential system. We propose to use the formalism of multiplicative strain decomposition, often used for plasticity or morphoelastic descriptions of growth [44] but which has also proven useful e.g. to model anisotropic solid viscoelastic tissues [64]. We show that this allows to define a tractable resolution procedure for large deformations.

Appendix A: Asymptotic Analysis of the Dynamics of the Unbound Chains

We choose the characteristic time $\tau_b = k_\mathrm{b}^{-1}$, and nondimensionalise with $\underset{\approx}{\boldsymbol{\ell}} = \overline{\underset{\approx}{\boldsymbol{\ell}}}/\tau_b$, and $\underset{\sim}{\boldsymbol{r}} = \beta^{-1}\overline{\underset{\sim}{\boldsymbol{r}}}$. Then (5b) writes:

$$\frac{\partial \psi_\mathrm{u}}{\partial \bar{t}} + \underset{\sim}{\nabla}_{\bar{\boldsymbol{r}}} \cdot \left(\psi_\mathrm{u} \overline{\underset{\approx}{\boldsymbol{\ell}}} \cdot \overline{\underset{\sim}{\boldsymbol{r}}} - \frac{\tau_b \kappa}{\zeta} \psi_\mathrm{u} \overline{\underset{\sim}{\boldsymbol{r}}} - \frac{\tau_b k_B T \beta^2}{\zeta} \underset{\sim}{\nabla}_{\bar{\boldsymbol{r}}} \psi_\mathrm{u} \right) = \tau_b k_\mathrm{u} \mathcal{K}_u(\psi_\mathrm{u}, \psi_\mathrm{b})$$

noting that $\kappa = k_B T \beta^2$, this can be rearranged as:

$$\underset{\sim}{\nabla}_{\bar{\boldsymbol{r}}} \cdot (\psi_\mathrm{u} \overline{\underset{\sim}{\boldsymbol{r}}} + \underset{\sim}{\nabla}_{\bar{\boldsymbol{r}}} \psi_\mathrm{u}) = \frac{\zeta}{\tau_b \kappa} \left(\frac{\partial \psi_\mathrm{u}}{\partial \bar{t}} + \underset{\sim}{\nabla}_{\bar{\boldsymbol{r}}} \cdot (\psi_\mathrm{u} \overline{\underset{\approx}{\boldsymbol{\ell}}} \cdot \overline{\underset{\sim}{\boldsymbol{r}}}) - \tau_b k_\mathrm{u} \mathcal{K}_u(\psi_\mathrm{u}, \psi_\mathrm{b}) \right)$$

Here the nondimensional number $\zeta/(\tau_b \kappa)$ compares the rate of binding $k_\mathrm{b} = 1/\tau_b$ to the rate of equilibration of spring and Brownian forces in unbound chains, κ/ζ. We assume that this number is vanishingly small. We also assume that $\tau_b k_\mathrm{u} \mathcal{K}_u$ and $\overline{\underset{\approx}{\boldsymbol{\ell}}}$ are of order 1 at most, we come back to these assumptions below. Then we can expand $\psi_\mathrm{u}(\underset{\sim}{\boldsymbol{r}}, t) = a_\mathrm{u}(t)\psi_0(\underset{\sim}{\boldsymbol{r}}) + (\zeta/(\tau_b\kappa))\psi'_\mathrm{u}(\underset{\sim}{\boldsymbol{r}}, t)$, where $a_\mathrm{u} = \int_{\mathbb{R}^3} \psi_\mathrm{u} \, \mathrm{d}\boldsymbol{r}$ and the constant distribution $\psi_0(\underset{\sim}{\boldsymbol{r}})$ is such that $-\kappa \psi_0 \underset{\sim}{\boldsymbol{r}} - k_B T \underset{\sim}{\nabla}_{\boldsymbol{r}} \psi_0 = \underset{\sim}{\boldsymbol{0}}$, thus solving the left-hand side,

$$\psi_0 = (\kappa/(2\pi k_B T))^{3/2} \exp(-\kappa \boldsymbol{r}^2/(2k_B T)).$$

The deviation ψ'_u solves:

$$\begin{aligned} \underset{\sim}{\nabla}_{\bar{\boldsymbol{r}}} \cdot (\psi'_\mathrm{u} \overline{\underset{\sim}{\boldsymbol{r}}} + \underset{\sim}{\nabla}_{\bar{\boldsymbol{r}}} \psi'_\mathrm{u}) = {} & \frac{\partial a_\mathrm{u}}{\partial \bar{t}} \psi_0 + \underset{\sim}{\nabla}_{\bar{\boldsymbol{r}}} \cdot (\psi_0 \overline{\underset{\approx}{\boldsymbol{\ell}}} \cdot \overline{\underset{\sim}{\boldsymbol{r}}}) - \tau_b k_\mathrm{u} \mathcal{K}_u \left(\psi_0 + \frac{\zeta}{\tau_b \kappa} \psi'_\mathrm{u}, \psi_\mathrm{b} \right) \\ & + \frac{\zeta}{\tau_b \kappa} \underset{\sim}{\nabla}_{\bar{\boldsymbol{r}}} \cdot (\psi'_\mathrm{u} \overline{\underset{\approx}{\boldsymbol{\ell}}} \cdot \overline{\underset{\sim}{\boldsymbol{r}}}). \end{aligned}$$

Integrating over $\mathbb{R}^3$, noting that ψ'_u integrates to zero and using the divergence theorem,

$$\frac{\partial a_\mathrm{u}}{\partial \bar{t}} = \tau_b k_\mathrm{u} \int_{\mathbb{R}^3} \mathcal{K}_u(\psi_\mathrm{u}, \psi_\mathrm{b}) \, \mathrm{d}\bar{\boldsymbol{r}}.$$

Since we have chosen $\mathcal{K}_u = \psi_\mathrm{b} - (k_\mathrm{b}/k_\mathrm{u})\psi_\mathrm{u}$, and $\int_{\mathbb{R}^3} \psi_\mathrm{b} \, \mathrm{d}\bar{\boldsymbol{r}} = 1 - a_\mathrm{u}$, we obtain

$$a_\mathrm{u}(t) = \frac{k_\mathrm{u}}{k_\mathrm{b} + k_\mathrm{u}} + a_\mathrm{u}^0 \exp(-(k_\mathrm{u} + k_\mathrm{b})t)$$

where $a_\mathrm{u}^0 = a_\mathrm{u}(0) - k_\mathrm{u}/(k_\mathrm{b} + k_\mathrm{u})$. Thus, after a transient, a_u is a constant and ψ'_u is such that

$$\underset{\sim}{\nabla}_{\bar{\boldsymbol{r}}} \cdot (\psi'_\mathrm{u} \overline{\underset{\sim}{\boldsymbol{r}}} + \underset{\sim}{\nabla}_{\bar{\boldsymbol{r}}} \psi'_\mathrm{u}) = \underset{\sim}{\nabla}_{\bar{\boldsymbol{r}}} \cdot (\psi_0 \overline{\underset{\approx}{\boldsymbol{\ell}}} \cdot \overline{\underset{\sim}{\boldsymbol{r}}}) - \tau_b k_\mathrm{u} \mathcal{K}_0(\psi_\mathrm{b}) + O\left(\frac{\zeta}{\tau_b \kappa} \right)$$

with $\mathcal{K}_0(\psi_\mathrm{b}) = \psi_\mathrm{b} - (k_\mathrm{b}/k_\mathrm{u})\psi_0$ and is at most of order 1 if $\max\{\overline{\underset{\approx}{\boldsymbol{\ell}}}, k_\mathrm{u}/k_\mathrm{b}\}$ is. Finally, this asymptotic development is valid for $\max\{|\underset{\approx}{\boldsymbol{\ell}}|, k_\mathrm{u}\} \lesssim k_\mathrm{b} \ll \kappa/\zeta$. The transient is of duration at most $1/k_\mathrm{b}$, thus shorter than the flow characteristic time $1/|\underset{\approx}{\boldsymbol{\ell}}|$.

Appendix B: Diffusive Molecular Motors

In Sect. 2.3 we assume that molecular motors can sense a directionality in the network and follow the oriented vector $\underset{\sim}{\boldsymbol{r}}$. This corresponds to the behaviour of myosin minifilaments on actin networks, however this may not be the case of all contractile biopolymer networks. Starting again from Eqs. (11a)–(11b), it is possible to construct another vectorial reaction coefficient based on the gradient of ψ_b, i.e. for any orientation tensor $\underset{\approx}{\mathbf{q}}$, specify $\underset{\sim}{\boldsymbol{j}}_\mathrm{a}$ such that it will yield a diffusion term in (6):

$$\lambda_{12}^{\mathrm{diff}} = -\frac{k_\mathrm{a}\theta^{\mathrm{diff}}}{\kappa}\underset{\approx}{\mathbf{q}}\cdot\underset{\sim}{\nabla}_{\boldsymbol{r}}\log\psi_\mathrm{b}, \qquad \underset{\sim}{\boldsymbol{j}}_\mathrm{a}^{\mathrm{diff}} = -\frac{k_\mathrm{a}\theta^{\mathrm{diff}}\Delta\mu}{\kappa}\underset{\approx}{\mathbf{q}}\cdot\underset{\sim}{\nabla}_{\boldsymbol{r}}\log\psi_\mathrm{b} - \frac{1}{2}k_\mathrm{s}\underset{\sim}{\boldsymbol{r}},$$
$$\dot{\xi}_\mathrm{a}^{\mathrm{diff}} = 2k_\mathrm{a}\underset{\sim}{\boldsymbol{r}}\cdot\underset{\approx}{\mathbf{q}}\underset{\sim}{\nabla}_{\boldsymbol{r}}\log\psi_\mathrm{b} + \lambda_{22}^{\mathrm{diff}}\Delta\mu,$$

where k_a is a typical rate of motor progression and θ^{diff} a numeric constant. As in the case of processive motors, we have taken $\lambda_{11} = k_\mathrm{s}/(2\kappa)$. In [28], we argue that the resulting diffusion term in Eq. (6) must scale with the square of the size of the steps ℓ_m that the molecular motors perform on the strands, thus $\theta^{\mathrm{diff}} = \ell_\mathrm{m}^2\beta^2$. Additionally, we can identify that $v_\mathrm{a} = \ell_\mathrm{m}k_\mathrm{a}$, where v_a was defined in Sect. 2.3 and found to be equal to $\ell_\mathrm{a}(k_\mathrm{u}+k_\mathrm{s})$. Evaluating $\lambda_{22}^{\mathrm{diff}}$ is more difficult than λ_{22} in the processive case, however taking ψ_b to be a small deviation from ψ_0, we find $\lambda_{22}^{\mathrm{diff}} > 3((k_\mathrm{u}+k_\mathrm{s})\ell_\mathrm{a}\ell_\mathrm{m}\beta^2)^2/(16\pi k_\mathrm{s}k_B T)$.

If we choose $\underset{\approx}{\mathbf{q}} = \underset{\approx}{\mathbf{I}}$, since $\langle\underset{\sim}{\boldsymbol{r}}\underset{\sim}{\nabla}_{\boldsymbol{r}}\log\psi_\mathrm{b}\rangle_\mathrm{b} = -\frac{k_\mathrm{b}a_\mathrm{u}}{k_\mathrm{u}}\underset{\approx}{\mathbf{I}}$, the contractility tensor is:

$$\underset{\approx}{\mathbf{A}}_\mathrm{a} = \frac{2\ell_\mathrm{a}\ell_\mathrm{m}\beta^2k_\mathrm{b}a_\mathrm{u}\Delta\mu}{k_\mathrm{u}\kappa}\underset{\approx}{\mathbf{I}}.$$

However the lack of alignment of the velocity $\underset{\sim}{\boldsymbol{j}}_\mathrm{a}$ with the microstructure is difficult to interpret. Following [28], it is also possible to take $\underset{\approx}{\mathbf{q}} = \underset{\approx}{\mathbf{Q}}$, which means that the diffusive-like behaviour of the molecular motors takes place along the direction of the strands $\underset{\sim}{\boldsymbol{r}}/|\underset{\sim}{\boldsymbol{r}}|$. Thanks to the property $\langle\underset{\sim}{\boldsymbol{r}}\underset{\approx}{\mathbf{Q}}\underset{\sim}{\nabla}_{\boldsymbol{r}}\log\psi_\mathrm{b}\rangle_\mathrm{b} = -\langle\underset{\approx}{\mathbf{Q}}\rangle_\mathrm{b}$, as above, and to the fact that $\mathrm{tr}\,\underset{\approx}{\mathbf{Q}} = 1$, we have

$$\underset{\approx}{\mathbf{A}}_\mathrm{a} = \frac{2\ell_\mathrm{a}\ell_\mathrm{m}\beta^2\Delta\mu}{\kappa}\langle\underset{\approx}{\mathbf{Q}}\rangle_\mathrm{b}.$$

Thus we find that the "diffusive" and "processive" types of reactive flux $\underset{\sim}{\boldsymbol{j}}_\mathrm{a}$ lead to expressions of the active stress which are highly similar.

Appendix C: Lower Bound on the Trace of the Microstructure Tensor

We show here that for appropriate initial conditions, and in particular $\underset{\approx}{\mathbf{A}}(t=0) = \underset{\approx}{\mathbf{A}}_0$, the trace of $\underset{\approx}{\mathbf{A}}$ remains larger than the one of $\underset{\approx}{\mathbf{A}}_0$. We use the fact that the material is incompressible ($\underset{\sim}{\nabla}_{\boldsymbol{x}}\cdot\underset{\sim}{\boldsymbol{v}} = 0$) and impose that $\underset{\approx}{\mathbf{A}}_\mathrm{a}$ is positive semi-definite, hence corresponds to a contractile active term. As stated in the main text, we essentially follow the proof of Lemma 2.1 by [38] but take into account the additional active term.

The modified lemma claims: assume that $\det\underset{\approx}{\mathbf{B}}(t=0) \geq 1$ and $\tau\overset{\triangledown}{\underset{\approx}{\mathbf{B}}} = -\underset{\approx}{\mathbf{B}} + \underset{\approx}{\mathbf{I}} + \underset{\approx}{\mathbf{B}}_a(t)$ with $\underset{\approx}{\mathbf{B}}_a(t)$ a symmetric semi-definite tensor. Then, $\forall t > 0$, $\det\underset{\approx}{\mathbf{B}}(t) \geq 1$. We apply this lemma with $\tau = k_\mathrm{u}^{-1}$, $\underset{\approx}{\mathbf{B}} = \beta^2a_0^{-1}\underset{\approx}{\mathbf{A}}$ and $\underset{\approx}{\mathbf{B}}_a = \beta^2a_0^{-1}\underset{\approx}{\mathbf{A}}_\mathrm{a}$, which matches the conditions of (17). Note

that both are indeed symmetric semi-definite by construction, since $\underset{\approx}{\mathbf{A}} = \langle \underset{\sim}{\boldsymbol{r}}\underset{\sim}{\boldsymbol{r}} \rangle_{\mathrm{b}}$ and $\underset{\approx}{\mathbf{A}}_{\mathrm{a}} = \frac{2\ell_a \beta \Delta\mu}{\kappa} \langle \frac{\underset{\sim}{\boldsymbol{r}}\underset{\sim}{\boldsymbol{r}}}{r^2} \rangle_{\mathrm{b}}$. The condition $\det(\underset{\approx}{\mathbf{B}}(t=0)) \geq 1$ is equivalent to $\det(\underset{\approx}{\mathbf{A}}(t=0)) \geq \det(\underset{\approx}{\mathbf{A}}_0)$.

Following [38], we observe that using Jacobi's formula, and for incompressible flow ($\mathrm{tr}\, \underset{\approx}{\boldsymbol{\ell}} = 0$),

$$\tau \frac{\partial \ln(\det(\underset{\approx}{\mathbf{B}}))}{\partial t} + \tau \underset{\sim}{\boldsymbol{v}} \cdot \underset{\sim}{\nabla}_{\boldsymbol{x}} \ln(\det(\underset{\approx}{\mathbf{B}})) = \underbrace{\tau\, \mathrm{tr}\left(\underset{\approx}{\boldsymbol{\ell}} + \underset{\approx}{\boldsymbol{\ell}}^{\mathsf{T}}\right)}_{=0} + \mathrm{tr}\left(-\underset{\approx}{\mathbf{I}} + \underset{\approx}{\mathbf{B}}^{-1} + \underset{\approx}{\mathbf{B}}^{-1}\underset{\approx}{\mathbf{B}}_a\right)$$

We use the inequality of arithmetic and geometric means applied to the non-negative eigenvalues of $\underset{\approx}{\mathbf{B}}^{-1}$ and $\underset{\approx}{\mathbf{B}}^{-1}\underset{\approx}{\mathbf{B}}_a$,

$$\frac{1}{3}\,\mathrm{tr}\,\underset{\approx}{\mathbf{M}} \geq (\det \underset{\approx}{\mathbf{M}})^{1/3},$$

and, introducing the derivative $\frac{\mathrm{d}}{\mathrm{d}t}$ along flow characteristics, obtain

$$\begin{aligned} \frac{\tau}{3} \frac{\mathrm{d} \ln(\det(\underset{\approx}{\mathbf{B}}))}{\mathrm{d}t} &\geq -1 + \det(\underset{\approx}{\mathbf{B}})^{-1/3} \left(1 + \det(\underset{\approx}{\mathbf{B}}_a)^{1/3}\right) \\ &\geq -1 + \det(\underset{\approx}{\mathbf{B}})^{-1/3} \end{aligned}$$

Setting $z = 1 - \det(\underset{\approx}{\mathbf{B}})^{1/3}$, we find $z(0) \leq 0$ and $\tau \frac{\mathrm{d}z}{\mathrm{d}t} \leq -z$, thus $z(t) \leq z(0) e^{-t/\tau}$ and $\det(\underset{\approx}{\mathbf{B}}(t)) \geq 1$.

Using the above upper bound of the determinant,

$$\mathrm{tr}\,\underset{\approx}{\mathbf{A}}_0 \leq 3 a_0 \beta^{-2} \det(\beta^2 a_0^{-1} \underset{\approx}{\mathbf{A}})^{1/3} \leq \mathrm{tr}\,\underset{\approx}{\mathbf{A}}.$$

Acknowledgements J.E. is grateful to John Hinch, Claude Verdier and Atef Asnacios for their important contributions to his approach of this topic. The authors thank Alexander Erlich, Eric Bertin, Jonathan Fouchard, Catherine Quilliet and an anonymous reviewer for their helpful comments.

Author contributions J.E. conceived the research. J.E., A.J., and P.R. performed the research. J.E., A.J. and P.R. wrote the manuscript. All authors reviewed the manuscript.

Data Availability No datasets were generated or analysed during the current study.

Declarations

Competing interests The authors declare no competing interests.

References

1. Taber, L.A.: Biomechanics of growth, remodeling, and morphogenesis. Appl. Mech. Rev. **48**, 487–545 (1995)
2. Huxley, A.F.: Muscle structure and theories of contraction. Prog. Biophys. Biophys. Chem. **7**, 255–318 (1957)
3. Caruel, M., Truskinovsky, L.: Physics of muscle contraction. Rep. Prog. Phys. **81**, 036602 (2018)
4. Bray, D., White, J.G.: Cortical flow in animal cells. Sci. Mag. **239**, 883–888 (1988)
5. Mitchison, T.J., Cramer, L.P.: Actin-based cell motility and cell locomotion. Cell **84**, 371–379 (1996)
6. Recho, P., Putelat, T., Truskinovsky, L.: Contraction-driven cell motility. Phys. Rev. Lett. **111**, 108102 (2013)

7. Salbreux, G., Charras, G., Paluch, E.: Actin cortex mechanics and cellular morphogenesis. Trends Cell Biol. **22**, 536–545 (2012)
8. Nedelec, F.J., Surrey, T., Maggs, A.C., Leibler, S.: Self-organization of microtubules and motors. Nature **389**, 305–308 (1997)
9. Koenderink, G.H., Dogic, Z., Nakamura, F., Bendix, P.M., MacKintosh, F.C., Hartwig, J.H., Stossel, T.P., Weitz, D.A.: An active biopolymer network controlled by molecular motors. Proc. Natl. Acad. Sci. USA **106**, 15192–15197 (2009)
10. Stuhrmann, B., Soares e Silva, M., Depken, M., MacKintosh, F.C., Koenderink, G.H.: Nonequilibrium fluctuations of a remodeling in vitro cytoskeleton. Phys. Rev. E **86** (2012)
11. Dembo, M., Harlow, F.: Cell motion, contractile networks, and the physics of interpenetrating reactive flow. Biophys. J. **50**, 109–121 (1986)
12. Erlich, A., Étienne, J., Fouchard, J., Wyatt, T.: How dynamic prestress governs the shape of living systems, from the subcellular to tissue scale. Interface Focus **12**, 058101 (2022)
13. Fung, Y.C.: What are the residual stresses doing in our blood vessels? Ann. Biomed. Eng. **19**, 237–249 (1991)
14. Goriely, A., Vandiver, R.: On the mechanical stability of growing arteries. IMA J. Appl. Math. **75**, 549–570 (2010)
15. Kruse, K., Joanny, J.F., Jülicher, F., Prost, J., Sekimoto, K.: Generic theory of active polar gels: a paradigm for cytoskeletal dynamics. Eur. Phys. J. E **16**, 5–16 (2005)
16. Jülicher, F., Kruse, K., Prost, J., Joanny, J.-F.: Active behavior of the cytoskeleton. Phys. Rep. **449**, 3–28 (2007)
17. Marchetti, M.C., Joanny, J.F., Ramaswamy, S., Liverpool, T.B., Prost, J., Rao, M., Aditi Simha, R.: Hydrodynamics of soft active matter. Rev. Mod. Phys. **85**, 1143–1189 (2013)
18. Liverpool, T.B., Marchetti, M.C.: Rheology of active filament solutions. Phys. Rev. Lett. **97**, 520 (2006)
19. Ahmadi, A., Marchetti, M.C., Liverpool, T.B.: Hydrodynamics of isotropic and liquid crystalline active polymer solutions. Phys. Rev. E **74**, 520 (2006)
20. Hawkins, R.J., Liverpool, T.B.: Stress reorganization and response in active solids. Phys. Rev. Lett. **113** (2014)
21. Pujol, T., du Roure, O., Fermigier, M., Heuvingh, J.: Impact of branching on the elasticity of actin networks. Proc. Natl. Acad. Sci. USA **109**, 10364–10369 (2012)
22. Gardel, M.L., Shin, J.H., MacKintosh, F.C., Mahadevan, L., Matsudaira, P., Weitz, D.A.: Elastic behavior of cross-linked and bundled actin networks. Science **304**, 1301–1305 (2004)
23. Green, M.S., Tobolsky, A.V.: A new approach to the theory of relaxing polymeric media. J. Chem. Phys. **14**, 80–92 (1946)
24. Yamamoto, M.: The visco-elastic properties of network structure: I. General formalism. J. Phys. Soc. Jpn. **11**, 413–421 (1956)
25. Bird, R., Armstrong, R.C., Hassager, O.: Dynamics of Polymeric Liquids. Volume 2. Kinetic Theory. Wiley, New-York (1987)
26. Larson, R.G.: Constitutive Equations for Polymer Melts and Solutions. Chemical Engineering, Butterworth (1988)
27. Larson, R.G.: The Structure and Rheology of Complex Fluids. Topics Chem. Engng. Oxford Univ. Press (1999)
28. Étienne, J., Fouchard, J., Mitrossilis, D., Bufi, N., Durand-Smet, P., Asnacios, A.: Cells as liquid motors: mechanosensitivity emerges from collective dynamics of actomyosin cortex. Proc. Natl. Acad. Sci. USA **112**, 2740–2745 (2015)
29. Risken, H.: The Fokker-Planck Equation (1996)
30. Deshpande, V., DeSimone, A., McMeeking, R., Recho, P.: Chemo-mechanical model of a cell as a stochastic active gel. J. Mech. Phys. Solids **151**, 104381 (2021)
31. Aubouy, M., Jiang, J.A., Glazier, Y., Graner, F.: A texture tensor to quantify deformations. Granul. Matter **5**, 67–70 (2003)
32. Lipowsky, R., Liepelt, S.: Chemomechanical coupling of molecular motors: thermodynamics, network representations, and balance conditions. J. Stat. Phys. **130**, 39–67 (2008)
33. Jülicher, F., Ajdari, A., Prost, J.: Modeling molecular motors. Rev. Mod. Phys. **69**, 1269–1282 (1997)
34. de Groot, S.R., Mazur, P.: Non-equilibrium Thermodynamics. Dover, New-York (1984)
35. Hinch, J., Harlen, O.: Oldroyd B, and not A? J. Non-Newton. Fluid Mech. **298**, 104668 (2021)
36. Lodge, A.S.: A network theory of flow birefringence and stress in concentrated polymer solutions. Trans. Faraday Soc. **52**, 120 (1956)
37. Broedersz, C.P., Depken, M., Yao, N.Y., Pollak, M.R., Weitz, D.A., MacKintosh, F.C.: Cross-link governed dynamics of biopolymer networks. Phys. Rev. Lett. **105**, 238101 (2010)
38. Hu, D., Lelièvre, T.: New entropy estimates for the Oldroyd-b model and related models. Commun. Math. Sci. **5**, 909–916 (2007)

39. Dicko, M., Saramito, P., Blanchard, G.B., Lye, C.M., Sanson, B., Étienne, J.: Geometry can provide long-range mechanical guidance for embryogenesis. PLoS Comput. Biol. **13**, e1005443 (2017)
40. Jourdain, B., Lelièvre, T., Le Bris, C.: Existence of solution for a micro–macro model of polymeric fluid: the fene model. J. Funct. Anal. **209**, 162–193 (2004)
41. Roux, C., Duperray, A., Laurent, V.M., Michel, R., Peschetola, V., Verdier, C., Étienne, J.: Prediction of traction forces of motile cells. J. R. Soc. Interface Focus **6**, 20160042 (2016)
42. Recho, P., Truskinovsky, L.: An asymmetry between pushing and pulling for crawling cells. Phys. Rev. E **87**, 022720 (2013)
43. Saha, A., Nishikawa, M., Behrndt, M., Heisenberg, C.-P., Jülicher, F., Grill, S.W.: Determining physical properties of the cell cortex. Biophys. J. **110**, 1421–1429 (2016)
44. Lubarda, V.A.: Constitutive theories based on the multiplicative decomposition of deformation gradient: thermoelasticity, elastoplasticity, and biomechanics. Appl. Mech. Rev. **57**, 95–108 (2004)
45. Rodriguez, E.K., Hoger, A., McCulloch, A.D.: Stress-dependent finite growth in soft elastic tissues. J. Biomech. **27**, 455–467 (1994)
46. Goriely, A.: The Mathematics and Mechanics of Biological Growth. Interdisciplinary Applied Mathematics, vol. 45. Springer, Berlin (2017)
47. Fierling, J., John, A., Delorme, B., Torzynski, A., Blanchard, G.B., Lye, C.M., Popkova, A., Malandain, G., Sanson, B., Étienne, J., Marmottant, P., Quilliet, C., Rauzi, M.: Embryo-scale epithelial buckling forms a propagating furrow that initiates gastrulation. Nat. Commun. **13**, 859864 (2022)
48. Bergou, M., Audoly, B., Vouga, E., Wardetzky, M., Grinspun, E.: Discrete viscous threads. ACM Trans. Graph. **29**, 1–10 (2010)
49. Nestor-Bergmann, A., Blanchard, G.B., Hervieux, N., Fletcher, A.G., Étienne, J., Sanson, B.: Adhesion-regulated junction slippage controls cell intercalation dynamics in an apposed-cortex adhesion model. PLoS Comput. Biol. **18**, e1009812 (2022)
50. Alrashdi, M.A.H., Giusteri, G.G.: Evolution of local relaxed states and the modelling of viscoelastic fluids. Phys. Fluids. **36**(9), 093129 (2024)
51. Califano, F., Ciambella, J.: Viscoplastic simple shear at finite strains. Proc. R. Soc. A. **479**(14) (2023)
52. Katoh, K., Kano, Y., Masuda, M., Onishi, H., Fujiwara, K.: Isolation and contraction of the stress fiber. Mol. Biol. Cell **9**, 1919–1938 (1998)
53. Deguchi, S., Ohashi, T., Sato, M.: Tensile properties of single stress fibers isolated from cultured vascular smooth muscle cells. J. Biomech. **39**(14), 2603–2610 (2006)
54. Fage, F., Asnacios, S., Pluta, A., Richert, A., Vias, C., Fouchard, J., Enslen, H., Etienne, J., Callan-Jones, A., Thery, M., Pereira, D., Asnacios, A.: Disentangling the contributions of stress fibres and the unbundled actin meshwork to the anisotropy of cortical tension in response to cell shape. Preprint (2024)
55. O'Brien, L.E., Zegers, M.M.P., Mostov, K.E.: Building epithelial architecture: insights from three-dimensional culture models. Nat. Rev. Mol. Cell Biol. **3**, 531–537 (2002)
56. Kruse, K., Joanny, J.-F., Jülicher, F., Prost, J., Sekimoto, K.: Asters, vortices, and rotating spirals in active gels of polar filaments. Phys. Rev. Lett. **92**, 078101 (2004)
57. Trepat, X., Lenormand, G., Fredberg, J.J.: Universality in cell mechanics. Soft Matter **4**, 1750–1759 (2008)
58. Bonfanti, A., Fouchard, J., Khalilgharibi, N., Charras, G., Kabla, A.: A unified rheological model for cells and cellularised materials. R. Soc. Open Sci. **7**, 190920 (2020)
59. Khalilgharibi, N., Fouchard, J., Recho, P., Charras, G., Kabla, A.: The dynamic mechanical properties of cellularised aggregates. Curr. Opin. Cell Biol. **42**, 113–120 (2016)
60. Wyatt, T.P.J., Fouchard, J., Lisica, A., Khalilgharibi, N., Baum, B., Recho, P., Kabla, A.J., Charras, G.T.: Actomyosin controls planarity and folding of epithelia in response to compression. Nat. Mater. **19**, 109–117 (2020)
61. Tlili, S., Gay, C., Graner, F., Marcq, P., Molino, F., Saramito, P.: Colloquium: mechanical formalisms for tissue dynamics. Eur. Phys. J. E **38**, 533 (2015)
62. Ishihara, S., Marcq, P., Sugimura, K.: From cells to tissue: a continuum model of epithelial mechanics. Phys. Rev. E **96** (2017)
63. Bandil, P., Vernerey, F.J.: Continuum theory for confluent cell monolayers: interplay between cell growth, division, and intercalation. J. Mech. Phys. Solids **181**, 105443 (2023)
64. Ciambella, J., Lucci, G., Nardinocchi, P.: Anisotropic evolution of viscous strain in soft biological materials. Mech. Mater. **192**, 104976 (2024)